

Diffraction-Pattern Sampling for Automatic Pattern Recognition

GEORGE G. LENDARIS, MEMBER, IEEE,
AND GORDON L. STANLEY

Abstract—This paper describes diffraction-pattern sampling as a basis for automatic pattern recognition in photographic imagery; it covers: diffraction-pattern generation, diffraction-pattern/image-area relationships, diffraction-pattern sampling, algorithm development (using an interactive computer-graphic based facility), facility description, and experimental results which have been obtained over the last few years at General Motors' AC Electronics-Defense Research Laboratories, Santa Barbara, Calif.

Sampling the diffraction pattern results in a sample signature—a different one for each sampling geometry. The kinds of information obtainable from sample signatures are described, and considerations for developing algorithms based on such information are discussed.

A tutorial section is included for the purpose of giving the reader an intuitive feeling for the kinds of information contained in a diffraction pattern and how it relates to the original photographic imagery.

INTRODUCTION

THE PURPOSE of this paper is to demonstrate the utility of diffraction-pattern sampling for automatically classifying patterns in photographic transparencies.

An important step in the design of automatic recognition devices using diffraction-pattern sampling is for the designer to become intimately familiar with diffraction patterns and their relationships to the original photographs. Accordingly, an allied purpose of this paper is to help the reader develop an intuitive feeling for the information available in diffraction patterns and its relationship to patterns in the original photographs.

Once the designer has developed this familiarity, he can determine the features of the diffraction pattern which correspond to the features of the original photographic images which are important to the recognition task at hand. On the basis of this, he can design a sampling scheme which will preserve this information. His task then is to study the resulting sampled information (called a sample signature), and become familiar with its properties and how they relate to the diffraction pattern (and, ultimately, to the original photograph). With this as a basis, he can proceed

Manuscript received June 18, 1969; revised December 5, 1969. Essentially, this paper is the same as one presented, by invitation, at the Pattern Recognition Studies, Seminar-in-Depth, sponsored by the Pattern Recognition Society and the Society of Photo-Optical Instrumentation Engineers on June 10, 1969, New York, N. Y., and appears under the same title in the proceedings of that Seminar.

G. G. Lendaris was with AC Electronics-Defense Research Laboratories, General Motors Corporation, Santa Barbara, Calif. He is now with the Oregon Graduate Center, Beaverton, Ore. 97005.

G. L. Stanley is with the AC Electronics-Defense Research Laboratories, General Motors Corporation, Santa Barbara, Calif. 93015.

to develop means for automatically performing the recognition task on the basis of the sampled information.

The basic pattern-recognition system configuration against which the discussions in this paper are made is shown in Fig. 1. The preprocessor processes the photographic input, extracts what information it can, and passes this on to the decision processor (this could be a computer); the output of the decision processor is the desired classification.



Fig. 1. Pattern-recognition system configuration assumed in this paper.

Diffraction-pattern sampling is intended to serve as a preprocessor for such a system. The decision processor must then use this sampled information to arrive at the desired classification. We discuss certain aspects of the decision processor design, and cite some experimental results which demonstrate the utility of this approach.

This paper has two main sections. Section I is concerned with helping the reader develop an intuitive feeling for the information contained in a diffraction pattern and how it relates to the original photographic imagery. Section II-A describes various aspects of the diffraction-pattern sampling process, and Section II-B cites some experimental results.

I. DEVELOPING A FEELING FOR DIFFRACTION PATTERNS

As mentioned in the Introduction, one of our purposes here is to give the reader an intuitive feeling for interpreting diffraction patterns. Here we show the diffraction patterns of some basic input patterns and discuss them with this aim in mind. Accordingly, these discussions will not be rigorous; for details, the reader is referred to texts such as [1]–[3].

Diffracted Pattern Basics

As in [4],¹ we start the discussion by stating two well-known facts.

1) The Fraunhofer diffraction pattern of an aperture is the two-dimensional Fourier transform of the transmission function of that aperture.

¹ This was the first paper in which we described our use of diffraction-pattern sampling for automatic pattern recognition.

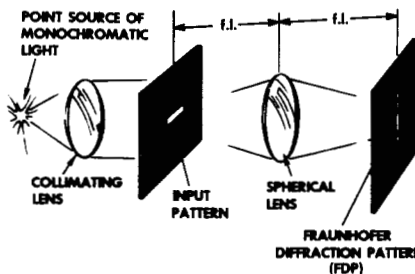


Fig. 2. FDP generation system.

2) Except for a linear phase factor, the Fourier transform of any function is independent of a translation of that function.

An optical configuration for generating the Fraunhofer diffraction pattern (FDP) of an input pattern is shown in Fig. 2.

Since the Fourier transform preserves rotation, if the input pattern is rotated, the FDP (which is centered on the optical axis of the system) is rotated about the optical axis but remains otherwise unchanged. We assume that the pattern given for identification is in the form of a photographic transparency, and call each portion of the transparency which is being "looked at" for identification a scan area (usually circular).

From 1) it follows that the FDP of a scan area is a spatial-frequency representation of the scan area. Since, however, physical sensors (such as the eye, film, photoelectric cells, etc.) sense the intensity (hence the phase factor of 2) disappears) and not simply the amplitude of a light distribution, the FDP as observed by these sensors is equivalent to the power spectrum² of the scan area's transmission function. To keep this distinction clear, in the remainder of this paper we will use FDPMS (FDP modulus squared) when referring to the FDP as it is photographed, as it is measured, or as we see it.

The center of the FDP corresponds to a spatial frequency of zero. Any other point in the plane of the FDP corresponds to a spatial frequency proportional to the points' distance from the origin and to the direction given by drawing a radius vector from the origin through that point. An intense high spatial-frequency indication along a given direction in the FDP corresponds to an object in the scan area with a small dimension in that direction. Similarly, an intense low-frequency indication along a given direction corresponds to an object with a large dimension in that direction. Further, the FDPMS is symmetric with respect to

the origin; that is, every intensity indication in the FDP has an identical counterpart which is located on the same direction line, on the other side of and the same distance from the origin.

A linear object in the original imagery gives rise to a distribution of light along a line centered on the optical axis. Similarly, a circular object gives rise to a distribution of light in concentric annular rings centered on the optical axis. Finally, a lattice-like object gives rise to lattice-like distribution of light in the diffraction pattern.

Single Simple Shapes

In Fig. 3(a) we show a simple rectangular aperture, and in Fig. 3(b), its FDPMS.

The intensity of the FDP along the direction corresponding to the width of the rectangle has the form $(\sin x/x)^2$, where $x = (\pi D/\lambda) \sin \alpha$, D is the width of the slit, λ is the wavelength of the (monochromatic) light used, and α is the angle between the optical axis and the line drawn from the lens center to the point x (in the focal plane). It follows that $x=0$ at the point where the optical axis intercepts the focal plane, and is the "center" of the FDP.

A semilogarithmic plot of the function $(\sin x/x)^2$ is shown in Fig. 4. The logarithm was chosen because it yields a better representation of what the eye perceives, e.g., Fig. 3(b). We note that the $(\sin x/x)$ function has its zeros at $x = \pi, 2\pi, 3\pi, \dots$; and from its definition, x takes on these values when $\sin \alpha$ takes on the values $\lambda/D, 2\lambda/D, 3\lambda/D, \dots$. Thus, the narrower the rectangle (smaller D), the wider the central lobe of the $(\sin x/x)^2$ curve and hence the FDPMS. Similarly, the wider the slit, the narrower the center portion of the FDPMS.

In Fig. 3(a), the length L of the rectangle is equal to $10D$. Therefore, the center lobe (and proportionately the rest) of the FDPMS (Fig. 3(b)) in the direction corresponding to the length of the rectangle is $1/10$ as large as in the direction corresponding to the width of the rectangle.

We next look at a circular aperture, Fig. 5(a). Fig. 5(b) is the FDPMS of a circular aperture of radius R , and Fig. 5(c) is the FDPMS of a circular aperture of radius $2R$ (these are called Airy disks).

Inasmuch as the 2-dimensional Fourier transform preserves circular symmetry, this FDPMS is circularly symmetric. The intensity as a function of radius r , measured from the optical axis, has the form $(J_1(r)/r)^2$ where $J_1(r)$ is a first-order Bessel function.

² During review it was suggested that the generality of the approach described in this paper might better be conveyed with the words "spatial-frequency power-spectrum sampling" rather than the words "diffraction-pattern sampling" since the fact that an optical system can be arranged to provide a Fourier transform is really incidental to the concepts involved. Consideration showed it would have been a major undertaking to make the necessary attendant changes throughout the paper. However, it is pointed out that the basic ideas expressed in this paper concerning FDPMSs apply to spatial-frequency power-spectra *in general*, no matter how they are obtained.

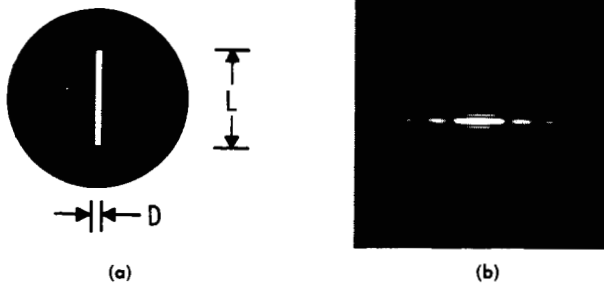
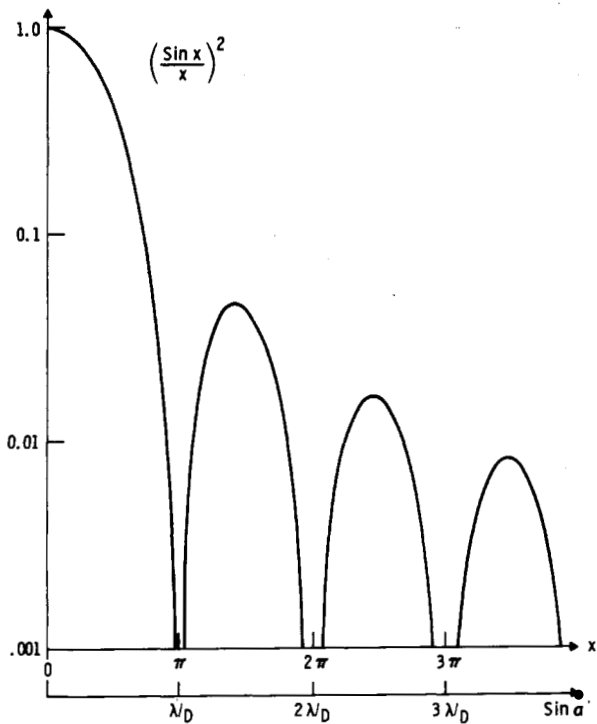


Fig. 3. (a) Rectangular aperture. (b) FDPMS of (a).

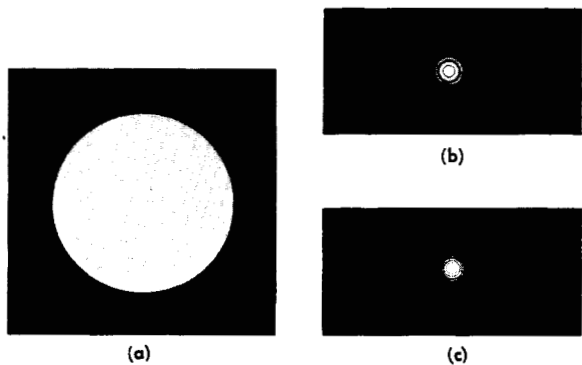
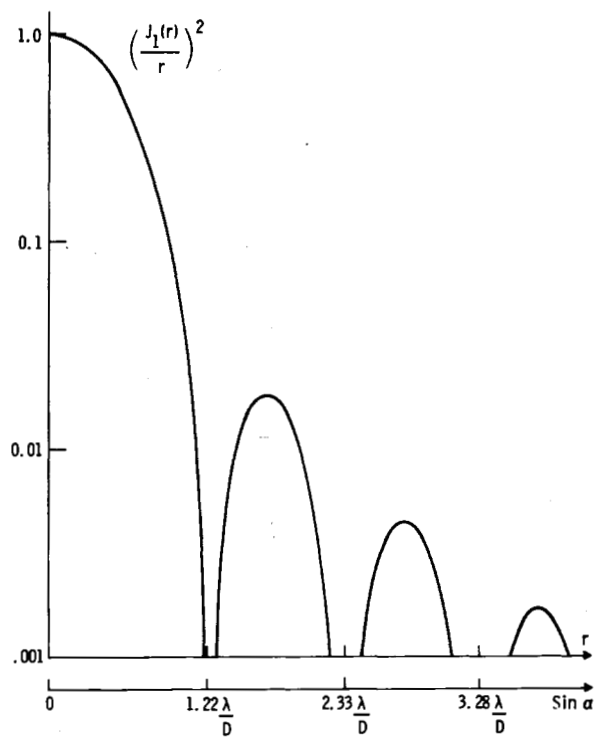
Fig. 4. Semilog plot of $(\sin x/x)^2$.

A semilogarithmic plot of the function $(J_1(r)/r)^2$ is shown in Fig. 6.

The relationships are not as straightforward as in the rectangular case, but it turns out that the zeros of this function occur at $1.22 \lambda/D, 2.33 \lambda/D, 3.238 \lambda/D \dots$. As in the rectangular case, the scaling of this function is inversely proportional to the diameter D of the circular aperture.

Multiple Simple Shapes

As a convenience in this paper, we will utilize the notions of impulse-sheets and two-dimensional impulses. An impulse-sheet has an infinite length in one direction (we call this the sheets' "direction"); its cross section, which remains the same along the sheets' entire length, has the usual delta-function properties. Multiplication of two intersecting impulse-sheets results in a single (two-dimensional) impulse located at the intersection of the two impulse-sheets.

Fig. 5. (a) Circular aperture. (b) FDPMS of (a) with radius R . (c) FDPMS of (a) with radius $2R$.Fig. 6. Semilog plot of $(J_1(r)/r)^2$.

The impulse-sheets and two-dimensional impulses have the following properties. (Since they are equivalent, we will use the term FDP instead of "two-dimensional Fourier transform.")

- 1) The FDP of an impulse-sheet is an impulse-sheet, centered at the origin and in a direction orthogonal to the direction of the original impulse-sheet.
- 2) The FDP of an infinite array of uniformly spaced parallel impulse-sheets is an infinite string of impulses along the direction orthogonal to the impulse-sheets' direction, with a spacing inversely proportional to the impulse-sheet separation, and with one of the impulses located at the origin.
- 3) Conversely, the FDP of a string of uniformly spaced impulses is an array of parallel impulse-sheets whose direction is orthogonal to the impulse string, whose separation is inversely proportional to the impulse

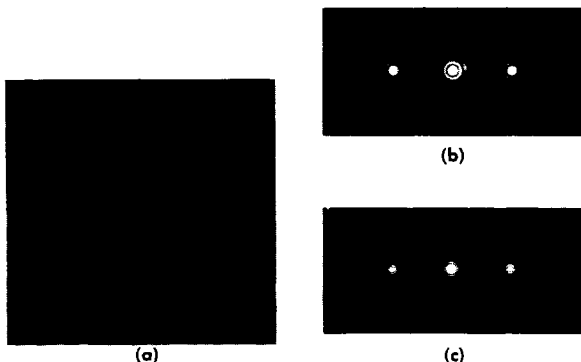


Fig. 7. (a) Parallel lines through a circular aperture. (b) FDPMS of a grating through radius R . (c) FDPMS of a grating through radius $2R$.

separation, and one of whose impulse-sheets goes through the origin.

- 4) The FDP of an infinite lattice-like array of impulses is an infinite lattice-like array of impulses whose dimensions are inversely related to those of the original lattice, with an impulse at the origin.
- 5) When convolving a function, call it y , with an array of impulses, the function y is simply replicated at the locations of each of the impulses.

Further, we will use the fact that the Fourier transform of a product of two functions is equal to the convolution of the Fourier transforms of the two functions; and, conversely, the Fourier transform of the convolution of two functions is equal to the product of the Fourier transforms of the two functions.

As an example, consider the scan area of Fig. 7(a). This is an array of uniformly spaced parallel straight lines as "seen" through a circular aperture. This scan area can be viewed as the result of multiplying an infinite array of parallel lines with the transmission function of the circular aperture. Therefore, to get the FDP of the combination, we convolve their two individual FDPs. The parallel lines are analogous to the parallel impulse-sheets noted earlier; therefore, by property 2), their FDP will be a string of impulses, with separation inversely related to the spacing of the lines and in a direction orthogonal to the lines. As previously noted, the FDP of the circular aperture is an Airy disk. Therefore, by property 5), the resulting FDP should consist of an Airy disk at the origin and at the locations of each of the remaining impulses (corresponding to the fundamental spatial frequency and all the harmonics which are present).

Fig. 7(b) and 7(c) is the FDPMSs of a grating as seen through the apertures which generated, respectively, Fig. 5(b) and 5(c). Note that in the FDPMSs, the replicated Airy disks have different sizes, corresponding inversely to the diameter of their respective circular apertures, while the replication positions, corresponding to the grating spacing, remain the same.

From a slightly different viewpoint, this can be seen as an analog of a sampled-data system. For this case, the parallel equally spaced linear apertures perform a "sampling" of the

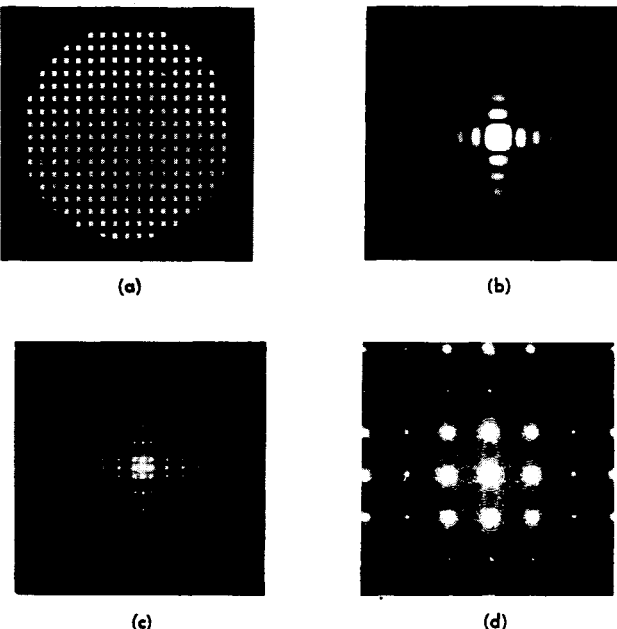


Fig. 8. (a) Array of rectangles through a circular aperture. (b) FDPMS of one of the rectangles of (a). (c) FDPMS of (a). (d) Center portion of (c).

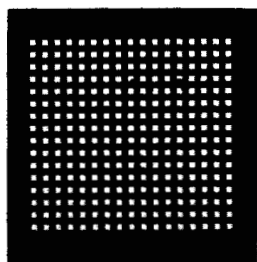
circular aperture function. As shown in sampling theory, in the frequency domain, the sampling operation introduces replications of the functions' spectrum at locations determined by the sampling frequency. Fig. 7(b) and 7(c) shows just exactly this situation.

As an example of multiple simple shapes, consider the configuration shown in Fig. 8(a). This is a two-dimensional array of identical rectangles as "seen" through a circular aperture. Three aspects of this array contribute to its FDP: the individual rectangle, the array geometry, and the scan aperture.

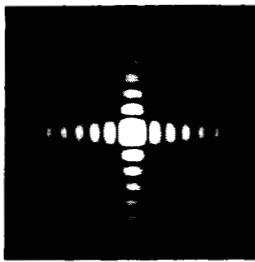
This array of rectangles can be viewed as the result of convolving one rectangle with an array of impulses (whose relative locations are the same as those of the array of Fig. 8(a)). Accordingly, the FDP of this array will be the product of the FDP of the rectangle and the FDP of the array of impulses. (Assuming this array to be infinite, then, by property 4), its FDP will also be an infinite array of impulses.)

The FDP of one of the rectangles of this array is shown in Fig. 8(b). Multiplying the FDP of the rectangle with the array of impulses yields what we may describe as a "sampled" FDP of the rectangle (where the "sampling" points are determined by the original array geometry and its dimensions). This is shown in Fig. 8(c).

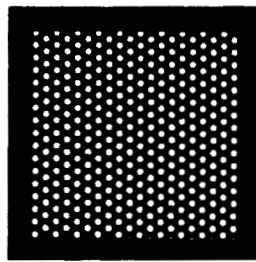
As with the previous example, Fig. 8(a) can be viewed as the product of the scan-area transmission function with that of an infinite array of rectangles. Again, this multiplication is equivalent to a convolution of the respective FDPs. Therefore, at each "sample point" of the FDP in Fig. 8(c) (up to this point, each of these is supposed to be an impulse) we should find replicated the FDP of the circular aperture. Since the aperture is much larger than the rectangles or the array dimensions, its FDP will be much smaller. The center



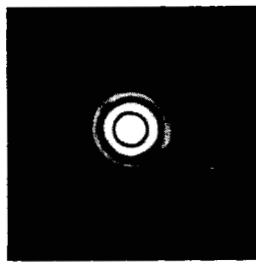
(a)



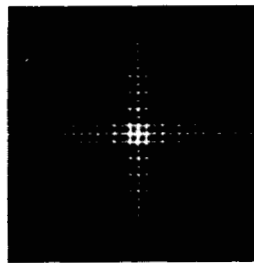
(b)



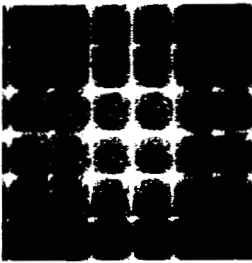
(c)



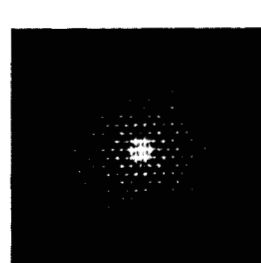
(d)



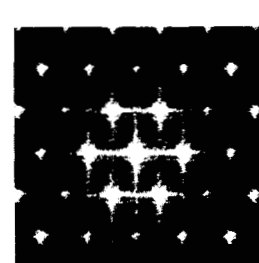
(a)



(b)

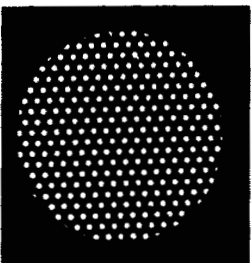


(c)

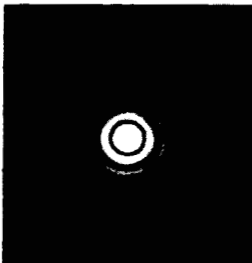


(d)

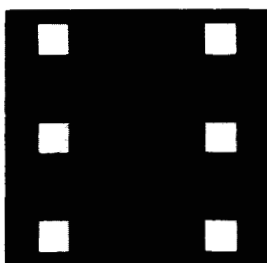
Fig. 9. (a) Array of rectangles through a rectangular aperture. (b) FDPMS of one of the rectangles of (a). (c) FDPMS of (a). (d) Center portion of (c).



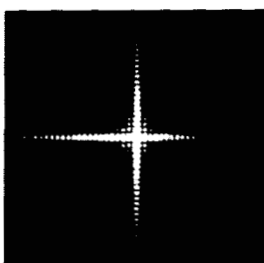
(a)



(b)

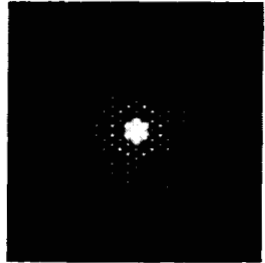


(c)

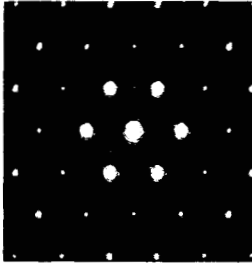


(d)

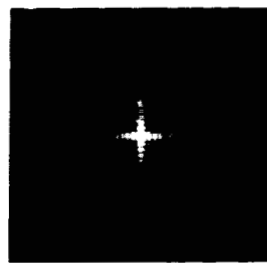
Fig. 11. (a) Array of circles through rectangular aperture. (b) FDPMS of one of the circles of (a). (c) FDPMS of (a). (d) Center portion of (c).



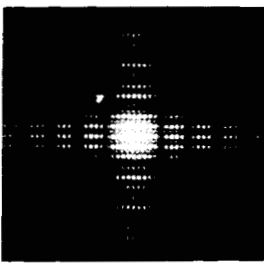
(a)



(b)



(c)



(d)

Fig. 12. (a) Array of six squares. (b) FDPMS of one of the squares of (a). (c) FDPMS of (a). (d) Center portion of (c).

of the Fig. 8(c) FDP is magnified in Fig. 8(d); we see there that the aperture FDP is in fact replicated at each "sample point."

This same discussion applies to Figs. 9 through 11, where in Fig. 9 we use a rectangular aperture; and in Figs. 10 and 11 we use an array of circles instead of rectangles.

In comparing these figures, we note that the circular aperture provides less visual contamination of the properties of the lattice than does the rectangular aperture (this would be

even more obvious if the rectangular aperture were rotated, say 45°). This is true in general, and for this reason, when scanning photographic images the circular aperture is generally preferred to a rectangular (or square) one.

As a less symmetrical example, consider the array of Fig. 12(a). This array can be viewed as the result of convolving one rectangle with an infinite array of impulses (whose vertical and horizontal spacings are as in Fig. 12(a)) and the result multiplied by an aperture to allow only the six squares

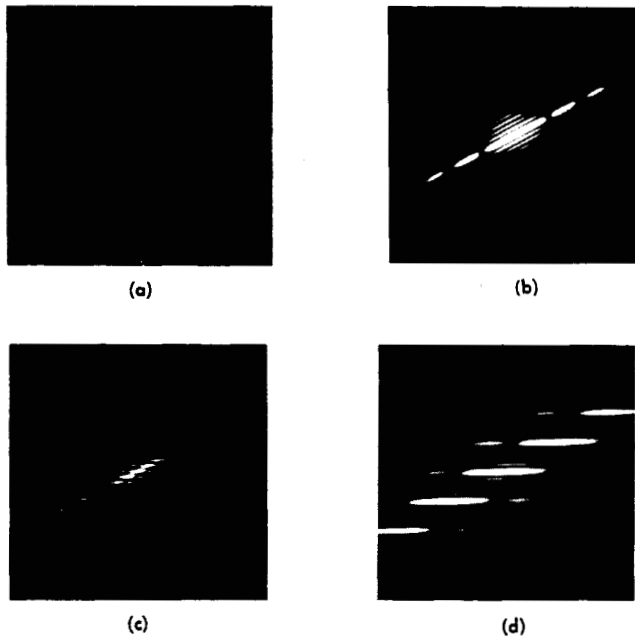


Fig. 13. (a) Staggered rectangular objects (similar to parked cars). (b) FDPMS of one of the rectangles of (a). (c) FDPMS of (a). (d) Center portion of (c).

of Fig. 12(a) to appear. The FDPMS of one of the rectangles is shown in Fig. 12(b). The result of multiplying this FDP with that of the impulse array is shown in Fig. 12(c) (again we have a "sampled" version of the Fig. 12(b) FDPMS). Note that the "sampling" points have a different spacing in the horizontal and vertical directions, corresponding to the differences in the respective spacings in the original array [Fig. 12(a)].

Whereas in the examples of Figs. 8 through 11 the aperture dimensions were considerably larger than the array dimensions, and therefore the FDPs of the aperture were considerably smaller than the spacings in the FDP array, in this example the aperture dimensions are nearly the same as those of the array. Therefore, the aperture FDP will be very noticeable as it is replicated at each of the array impulse locations. This is particularly noticeable in the vertical direction of Fig. 12(c), and as shown in the $5 \times$ magnification, Fig. 12(d). The lighter indications in the FDP are the second lobe (refer to Fig. 4) of the aperture FDP.

As a final example, consider the array of Fig. 13(a). This can be viewed as the result of convolving a small rectangle (oriented at approximately 60°) with a vertically oriented infinite string of uniformly spaced impulses, and the result multiplied by an aperture to limit its vertical extent. The FDPMS of one of the small rectangles is shown in Fig. 13(b). By property 3) the FDP of a vertically oriented string of uniformly spaced impulses is an infinite array of parallel horizontal impulse-sheets. Multiplying these two FDPs, we again obtain a "sampled" version of Fig. 13(b), shown in Fig. 13(c); only this time we have "sampling lines" instead of "sampling points." Further, the vertical component of the aperture's FDP will be replicated at each of the impulse-sheets (since the cross section of each of these impulse-

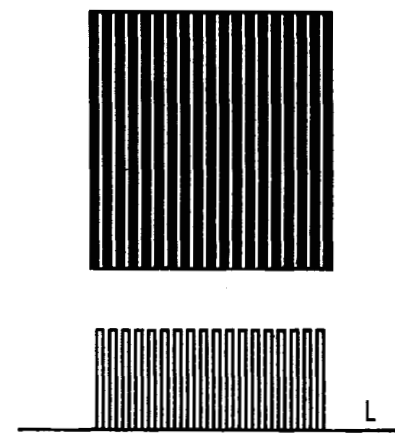


Fig. 14. Example of using projections to obtain FDP profile (along projection direction).

sheets has the usual impulse properties). These can be seen in Fig. 13(d), which is a $5 \times$ magnification of the center portion of Fig. 13(c).

Interpreting the FDP in Terms of Projections

Another convenient tool for looking at a scan area and getting a gross feeling for what its FDP will look like is briefly discussed next.

Assume that the pattern of interest has a transmission value of 1, and that of the background is 0. Strike a line L in any direction, but outside the scan area. Now perform a vertical projection (via a line integral) of the pattern onto the given line (as illustrated in Fig. 14). Take the (one-dimensional) Fourier transform of the resulting "signal" on the projection line, and this gives the profile of the FDP along that direction. (In the FDP, the direction line corresponding to each projection line passes through the origin.)

As a simple example, consider the scan area of Fig. 14. We see that the projection onto L is a "signal" consisting of a number of equally spaced pulses; in no other direction will the "signal" be periodic. Along the (horizontal) L direction then, we expect to see contributions at the locations corresponding to the period of the "signal" and at the locations corresponding to the harmonics of this (spatial) frequency that are present in the "signal." Along the other directions, no such components should be expected. This is a "quick and dirty" way of predicting the gross characteristics of the FDP we obtained in Fig. 7.

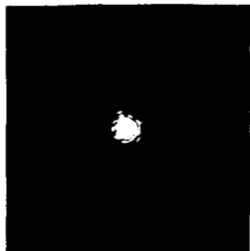
Scan-Area/FDPMSs from Aerial Photographs

An important fact to extract from all of the above examples is that every pattern in a scan area will have its own diffraction pattern, and each of these will be superimposed, centered on the optical axis. Accordingly, a building-block approach to interpreting the FDPs is useful, and the foregoing patterns can be considered as basic building blocks.

Figs. 15 through 26 are scan-area/FDPMS pairs taken from aerial photographs. The reader is invited to study



(a)



(b)

Fig. 15. (a) Natural terrain. (b) FDPMS of (a).



(a)



(b)

Fig. 16. (a) Roadway with natural terrain background. (b) FDPMS of (a).

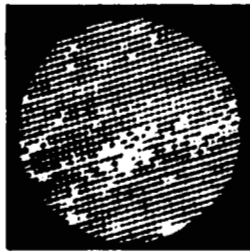


(a)



(b)

Fig. 17. (a) Road intersection. (b) FDPMS of (a).

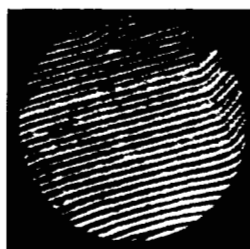


(a)



(b)

Fig. 18. (a) Orchard. (b) FDPMS of (a).

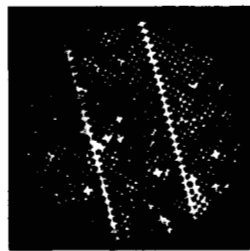


(a)

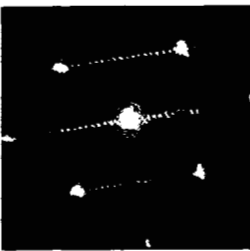


(b)

Fig. 19. (a) Orchard on hillside. (b) FDPMS of (a).



(a)



(b)

Fig. 20. (a) Orchard with service roads. (b) FDPMS of (a).

them, keeping in mind the basic information cited above, and the importance, mentioned earlier, of the designer developing an ability to interpret the FDP in terms of content of the scan area, for this will lead to an understanding of significant features in the sample signatures. The latter will be discussed in the next section.

II. SAMPLING DIFFRACTION PATTERNS

A. Description

Reason for Sampling

Although the process of going from a scan area to its FDP considerably reduces the complexity of the pattern recognition task, we are still dealing with a two-dimensional distribution of light. This will have to be converted to a form more convenient for subsequent processing.

As we noted earlier, the transformation of the scan area to its FDP is done in the preprocessor portion of the system (refer to Fig. 1). To perform its appropriate task, the preprocessor should reduce as much as possible the amount of information the decision processor has to handle.

Sampling is a good tool for further reducing the amount of information to be sent to the decision processor. The basic task is to design the sampling properly so that the resulting sampled data contain sufficient information for the subsequent classification to be effected. The FDP is particularly suited to sampling, because, as noted earlier, the scan area is decomposed into its basic building-block patterns, and the contribution of each of these to the FDP is centered on the optical axis of the system no matter where the pattern is located within the scan area. The optical axis, therefore, provides a reference point from which all sampling can be done. (No such reference point exists in the original scan area.) Due to this building block and centering property of the FDP, sampling geometries can be configured which are rotation invariant, size invariant, or both (depending on the subsequent processing). These are attractive features for a preprocessor to have.

The purpose, then, of sampling the FDP is to reduce this two-dimensional distribution of light to a relatively small set of numbers—called a sample signature.

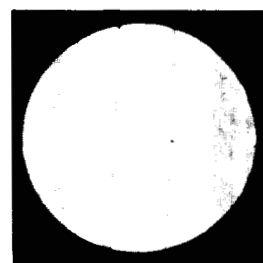


(a)

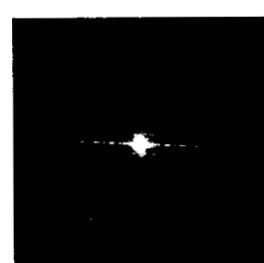


(b)

Fig. 21. (a) Vine crop. (b) FDPMS of (a).

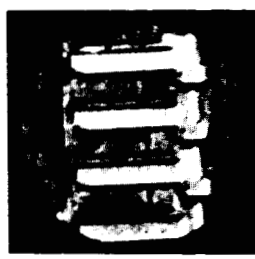


(a)

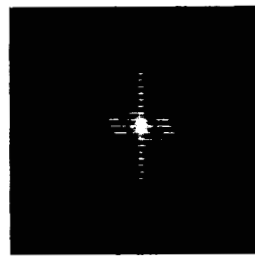


(b)

Fig. 24. (a) Runway strip with chevrons. (b) FDPMS of (a).

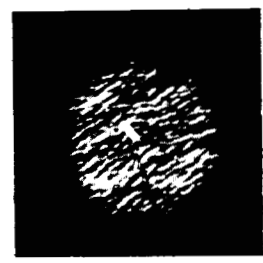


(a)



(b)

Fig. 22. (a) Complex of large buildings. (b) FDPMS of (a).



(a)

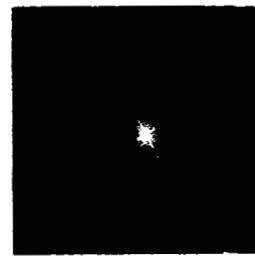


(b)

Fig. 25. (a) Ship at sea and wake. (b) FDPMS of (a).

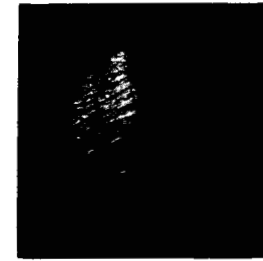


(a)

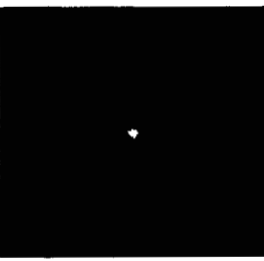


(b)

Fig. 23. (a) Complex of smaller buildings. (b) FDPMS of (a).



(a)



(b)

Fig. 26. (a) Ship wake and ocean surface. (b) FDPMS of (a).

Sampling Geometries

The process of sampling an FDP is basically one of measuring the amount of light energy falling within specified areas of the FDP. To do this, we define a set of areas, which, taken together, normally cover the FDP; we call this set of areas a "sampling geometry." Then we measure the total light energy falling within each area; we call the resulting set of measurements a sample signature. In principle, this sampling can be performed by constructing a physical set of sampling windows, one window for each of the defined areas. Each window is transparent over its corresponding sampling area, and opaque elsewhere. Each window is successively placed at the diffraction-pattern plane, and the light transmitted through the clear portion of the window is measured and converted to a number. The resulting numbers form the sample signature.

Because the sampling is done over two dimensions, there is a large variety of possible sampling geometries. A few of these possibilities intuitively hold promise for being especially useful in those cases where regularity of any kind is

present in the scan area (e.g., linear features, one- or two-dimensional periodicity, etc.). This is important, because man-made objects, in aerial photographs, for example, normally exhibit some kind of regularity.

For one of these possibilities, we recall that any point in the FDP plane corresponds to a frequency determined by its radial distance from the origin, and note that a circle in the FDP plane centered on the optical axis corresponds to one frequency in all directions. Therefore, by integrating the light energy of the diffraction pattern along a circle centered on the optical axis, we obtain the total contribution of one frequency component, independent of direction. In practice, an annular-ring sampling window will have a finite width [see Fig. 27(a)]; accordingly, each sampling window will obtain the contribution of a small number of adjacent frequencies. Having a finite width is advantageous, both because it helps to reduce the number of samples we have to take, and because it helps to make the sample signature insensitive to minute variations within the scan area (e.g., for noise considerations). A set of annular-ring

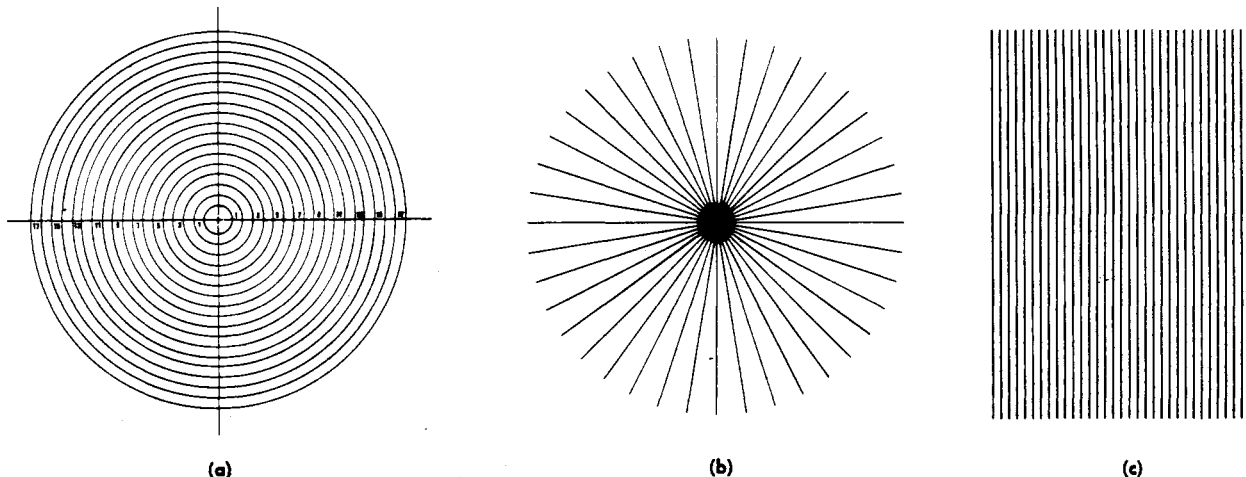


Fig. 27. (a) Annular-ring sampling geometry. (b) 9° wedge sampling geometry. (c) Parallel-slit sampling geometry.

sampling windows obtains a spatial-frequency profile of the contents of the scan area, and takes into account all directions simultaneously. (See Fig. 28(e) and 28(f) for examples of annular-ring sample signatures.) This technique of sampling provides a means for detecting one- or two-dimensional spatial periodicity within the scan area and, further, it is insensitive to rotation of the scan area.

For another sampling geometry, we recall that any point in the FDP plane corresponds to a direction (in the scan area) determined by drawing a radius vector from the origin through that point. Note that a radial line in the FDP plane corresponds to a single direction in the scan area, which includes all frequencies. Therefore, by integrating the light energy of the diffraction pattern along a radial line, we obtain the total contribution of one direction, independent of frequency (and independent of location in the scan area). In practice, a wedge-shaped sampling window is used [see Fig. 27(b)]. This obtains the contributions of a small number of adjacent directions, and has the advantages of reducing the number of samples required and reducing the effects of small variations. A set of wedge-shaped sampling windows obtains a direction profile of the contents of the scan area, and takes into account all frequencies simultaneously. (See Fig. 28(g) and 28(h) for examples of wedge sample signatures.) This technique of sampling is, grossly speaking, insensitive to scale.

Another possibility is what we call a parallel-slit sampling geometry. In this case, after rotating the FDP to a specified orientation, we measure the light energy transmitted through a slot of a specified width and long enough to cover the FDP. This sampling geometry is useful for distinguishing one-dimensional regularity from two-dimensional regularity. (The annular-ring geometry is used to detect the regularity and the wedges to find the principal directions. The slit is taken along these directions to distinguish the one-dimensional from the two-dimensional regularity.)

Finally, a frequency profile can be obtained along any desired direction by placing a very small aperture at, or near, the origin and moving it along the desired direction

radius; taking sufficient measurements to cover the line. (See Fig. 39 for example.)

A mathematical description of these sampling geometries is given in Appendix I.

Sample Signature Examples

Examples of sample signatures obtained via the annular-ring and wedge sampling geometries are given in Fig. 28.

FDP Sampling System

The implementation of diffraction-pattern sampling at General Motors' AC Defense Research Labs. (DRL) has undergone a two-step evolution from that described in [4]. The first of these implementations was used for two basic studies. The first study [5], performed on an aerial photograph of the Goleta Valley, Calif., was used to determine the feasibility of utilizing diffraction-pattern sampling as an aid to classifying areas in aerial photographs. The second study [6] was performed to determine to what extent dimensional information concerning the objects to be classified could be extracted from diffraction patterns. The results of these two studies were very encouraging; and in order to perform more in-depth studies of diffraction-pattern sampling, a fully automated Diffraction-Pattern Sampling System (DPSS) was built. The DPSS (shown in Fig. 29) provides for a wide variety of sampling geometries (important in a research environment), and for greater precision and higher sampling rates than either of our previous systems.

The DPSS is directly coupled to a large-scale computer and is controllable via a control station ⑤ or the General Motors developed Signature Analysis Research Facility (SARF) design console ⑥. The system basically operates as follows. A laser beam illuminates a selectable area of a photographic transparency mounted on an *X-Y* table ①, the diffraction pattern is formed optically, and can be sampled by the computer-controlled mechanisms at ②. In an alternate path, the diffraction pattern and/or the scan area of the photograph is observable by the analyst at either the viewing screen at ③ or the one at ④. When at ③, the analyst

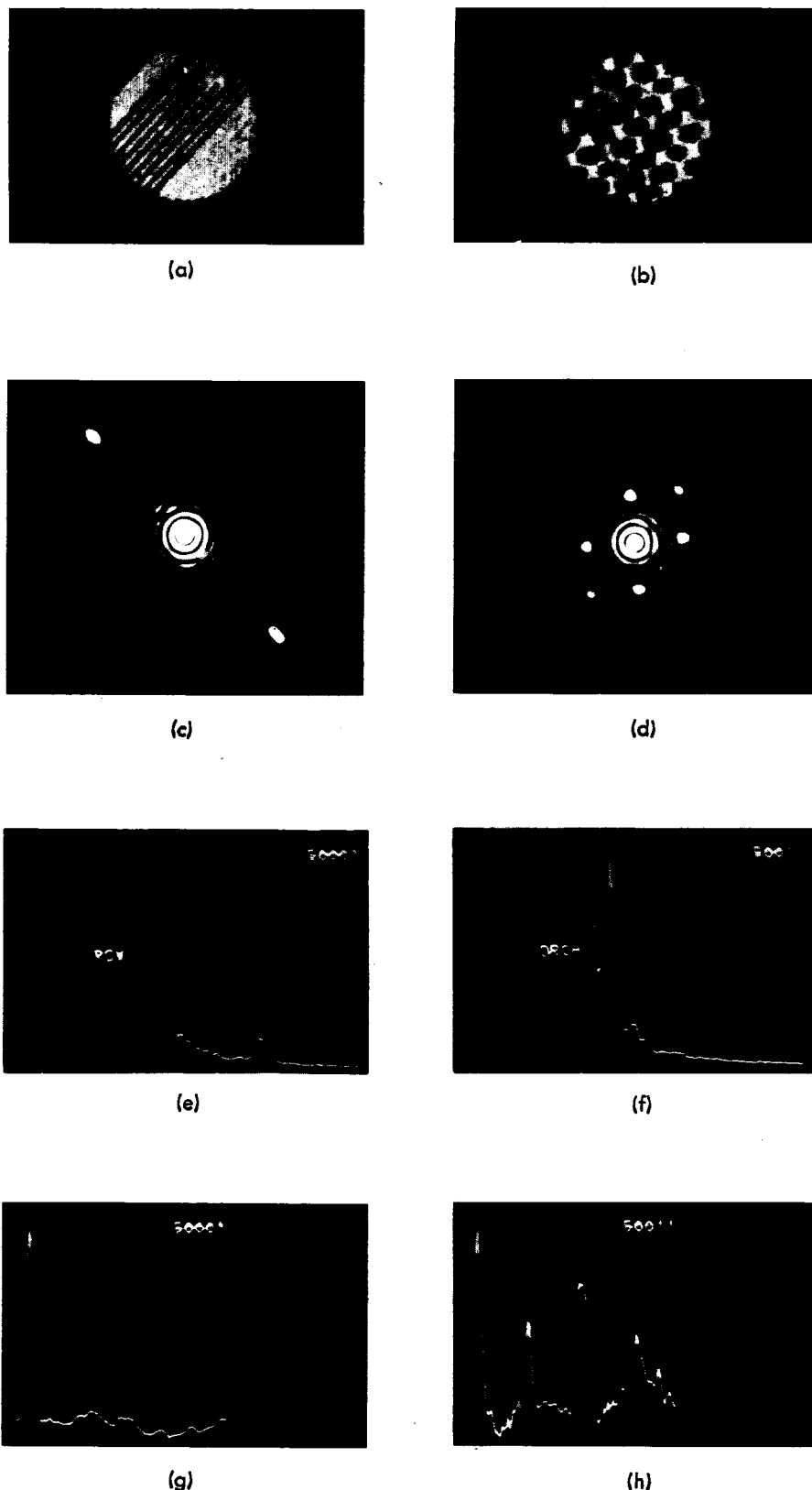


Fig. 28. (a) Agriculture one-dimensional periodicity. (b) Agriculture two-dimensional periodicity. (c) FDPMS of (a). (d) FDPMS of (b). (e) Annular-ring sample signature of (c). (f) Annular-ring sample signature of (d). (g) 1.8° wedge sample signature of (c). (h) 1.8° wedge sample signature of (d).

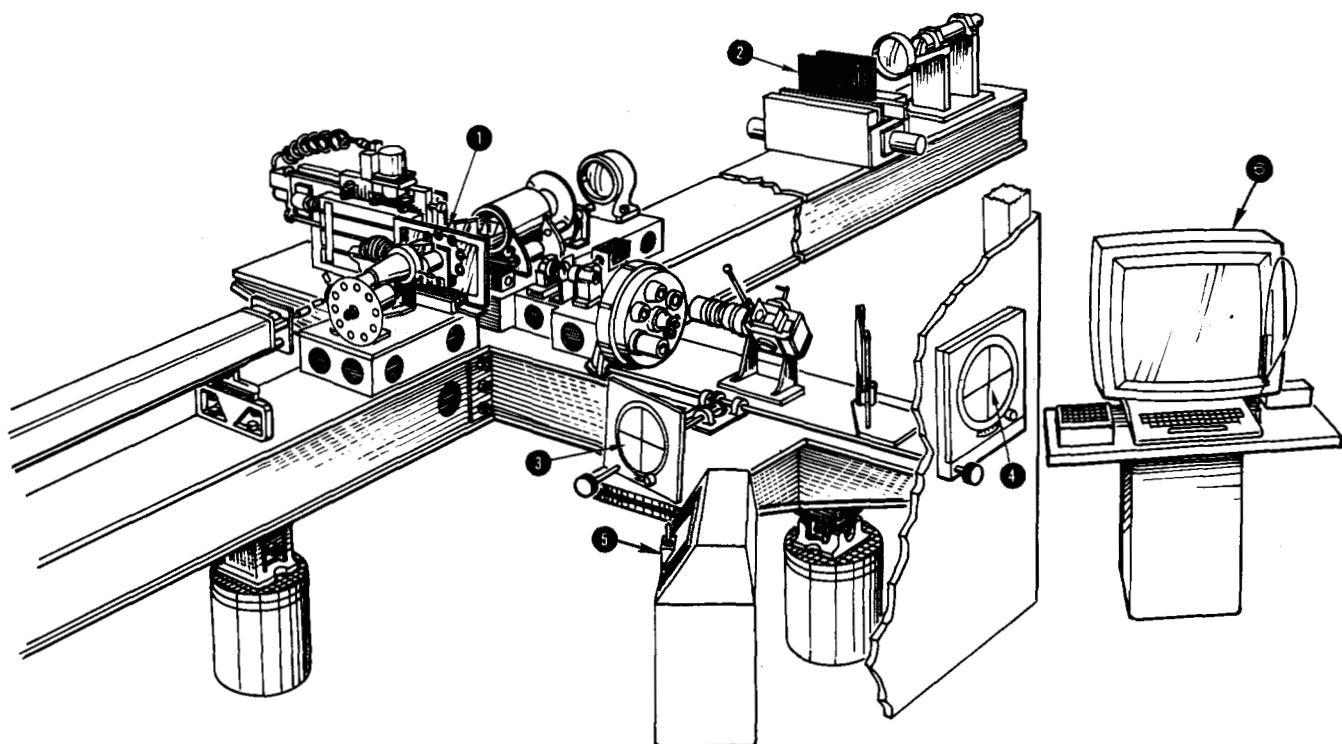


Fig. 29. Diffraction-pattern sampling system (DPSS).

can control the coordinates of the scan aperture using the joy stick at the control station (6) and can perform non-computer experiments. When at (4), the analyst can view the diffraction patterns and/or the scan areas, and can simultaneously view on the SARF graphics console (6) the sample signatures and any processing of the signatures he wishes to correlate with the diffraction pattern and/or the scan area while developing automatic classification algorithms.

A more detailed description of a DPSS is given in Appendix II.

Utilizing FDP Sample Signatures

As noted earlier, the purpose of sampling the FDP is to reduce the FDP to a representation consisting of a relatively small set of numbers. The next question is, how do we best use the resulting sample signatures?

In contrast to various "template matching" approaches, we treat the collection of numbers (which is the sample signature) as a "signal," or "signature" and plot it graphically. The human algorithm designer studies the signatures, discovers their distinguishing features, and devises schemes (algorithms) for machines to perform the classification task based on these features.

We noted earlier that the algorithm designer must become intimately familiar with the FDP and its relationships to the scan area so he can interpret the FDP in terms of important features of the scan area. Similarly, the designer must now study the sample signatures and become intimately familiar with their characteristics and how they relate to features of the FDP so that he will be able to arrive at the processing steps necessary to perform the pattern recognition task.

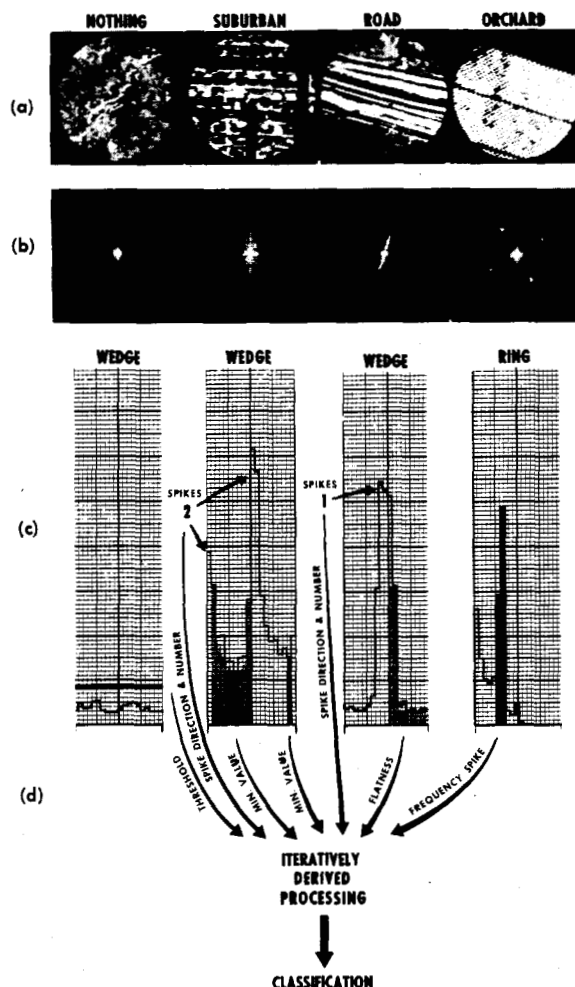


Fig. 30. Classification process.

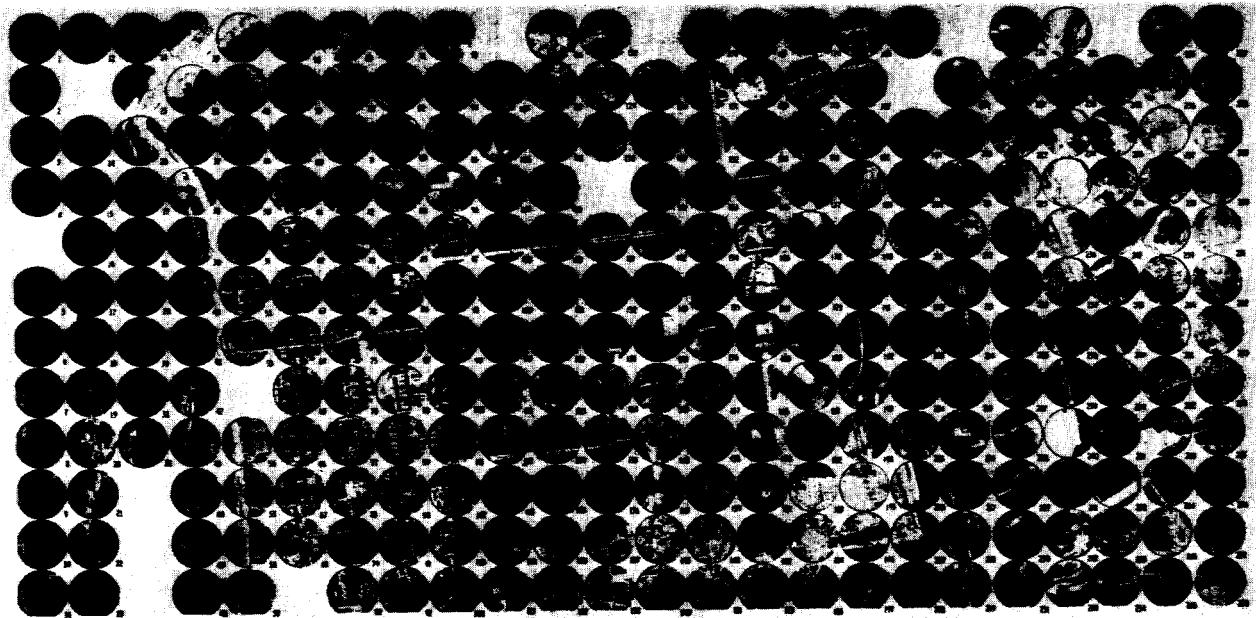


Fig. 31. Aerial photograph of Goleta Valley with scan-area selections indicated.

With reference to Fig. 30, our overall design approach can be stated as follows.

- 1) Studying (a) and (b), discover pertinent features in the FDP as related to content in the scan areas, and determine appropriate sampling geometries for the given task(s).
- 2) Studying (b) and (c), discover features in the sample signatures (and/or transformed versions of the signatures) which correspond to the FDP features discovered in 1), and determine appropriate data processing schemes for extracting measures of these features.
- 3) Iteratively arrive at decision procedures (d) utilizing these feature measures to perform the classification.

In practice, this design process has been found to be a highly intuitive and iterative process, and the "iteratively derived processing" represents the algorithm designer adapting as he interacts with the data and its processing.

SARF was developed by General Motors at AC-DRL to facilitate this "adaptive" design process (where we emphasize that the adaption is done by the algorithm designer). It is based on interactive computer graphics, and provides for real-time interaction between the designer, his data, and its processing, and is designed to take advantage of human intuition, judgment, and pattern discovery capabilities. It allows the designer to formulate hypotheses and to quickly test them, and, in particular, to utilize the exceptions or unexpected results of these tests. (SARF is described in [7]–[9].)

B. Experimental Results

The experimental results of this section are offered as examples of the utility of diffraction-pattern sampling for performing various aspects of automatic pattern recognition. The two algorithms described were developed only far enough to show a point, and have not been incorporated in any operational system.

When setting out to design an automatic pattern recognizer, we must first define the task to be performed. We define the work 'task' as looking for a specified object or class of objects in the given imagery. Associated with the objects of interest are certain physical constraints such as size and shape. These constraints determine the ground-distance diameter (GDD) of the scan-area aperture to be used for performing the task. In general, the smaller the object to be classified, the smaller the GDD required.

Goleta Valley Study

The main study performed on the second of the three implementations of a diffraction-pattern sampling system at AC-DRL was based on an aerial photograph of the Goleta Valley, Calif. [5]. This photograph included a ground area of roughly 1.7 by 3.4 miles, and, as shown in Fig. 31, was sectioned off into disjoint circular areas of 750 feet ground-distance diameter (these were the scan areas). The task was to classify each of these scan areas according to whether or not they displayed any gross man-made characteristics. Accordingly, two major classifications were defined: 1) gross man-made, and 2) nothing man-made. The gross man-made category was further divided into a) roads, b) intersections of roads, c) buildings, and d) orchards.

Since gross man-made characteristics were sought rather than small man-made objects—that is, for example, freeways and suburbia rather than small dirt roads and single dwellings—we choose a GDD of 750 feet. With this GDD, a road less than 20 feet wide could not be detected, for instance, (unless it was in strong contrast to the rest of the scan-area background and traversed approximately the center of the scan area) and a very large building, say 1000 feet on a side, would probably be misclassified.

Scan areas that contained more than one category were classified in the category whose features were most pro-

nounced. In this manner, no scan area was classified into more than one category.

The FDP of each of these scan areas was sampled via two sets of sampling windows. The first set consisted of 20 annular rings, and the second consisted of 20 nine-degree wedges. Classification parameters were derived from each of the resulting sample signatures; and these parameters (rather than the original sample signatures) were used in the subsequent classification process.

The initial set of classification parameters derived from the sample signatures were, in a sense, equivalent to the differences observed visually in the diffraction patterns. This first set provided a usable basis for deriving other parameters; and it was these that were used to effect the final classification algorithm of this study.

Features Utilized: The annular-ring sample signature for a scan area containing no regularity will fall off exponentially as a function of radius. (This statement assumes that the width of the annular-ring window is such that it cannot resolve the variations of the scan-aperture Airy disk.) If the scan area contains regularity, the energy in the FDP is redistributed and yields "bright" spots in certain areas of the FDP. The reading from the annular-ring window that coincides with such a bright spot will be higher than expected from the exponential fall-off model cited above. It turns out, then, that if an annular-ring window reading is equal to or larger than its neighbor on the low-frequency side, then the scan area can be assumed to have some kind of regularity. In particular, since orchard scan areas give rise to a lattice-like diffraction pattern, their annular sample signatures show sudden changes in the sampled value. This property alone allowed us to correctly classify the orchard scan areas in the Goleta Valley photograph with 100 percent accuracy.

The wedge sample signature is a good representation of those FDPs whose corresponding scan area contains linear images. Linear images in the scan area give rise to energy distributions along certain radii in the diffraction pattern, and these bright radii give rise to spikes in the wedge sample signature plot. The term "spike" refers to an abrupt rise in the sample signature plot, which in turn corresponds to a high intensity portion of the FDP impinging on a sample window [see Fig. 28(g) and (h) and Fig. (30)]. The number of these spikes, their angular relationship, and the distribution of energy between them, formed the basis upon which the remaining discriminations in this study were made.

Further details of the algorithm arrived at in this study are given in [5]. The classification results of the final algorithm for that study are given in Fig. 32.

San Francisco Bay Area Algorithm

Upon completion of the SARF and DPSS facilities described earlier, a demonstration algorithm was developed for distinguishing residential, agricultural, and natural areas in an aerial photograph of a portion of the San Francisco Bay Area [7]-[9].

This algorithm again demonstrated the utility of diffraction-pattern sampling for performing this kind of classifi-

	Actual	Hit	False Alarm	Hit (%)
NOTHING	108	93	2	86.1
MANMADE	167	165	15	98.8
False Rejection Rate				
$\frac{2}{167} = 1.2\%$				
Subclassification of MANMADE				
Buildings	37	36	10 ⁷¹ 3N	97.2
Roads	50	47	9 ^{9N} 1B	94.0
Inter-selections	35	28	1B 5 ^{1R} 3N	80.0
Orchards	45	45	0	100
TOTAL	167	156	24	93.4

Fig. 32. Summary of machine classification results for Goleta Valley study.

fication. More importantly, however, the development of this algorithm (and subsequent work done on the facility) demonstrated the rapidity with which such algorithms can be developed using a facility like SARF/DPSS.

For this algorithm, annular-ring and wedge sample signatures were again used—only this time, 100-point signatures instead of 20-point signatures were used.

These sample signatures were perused, and after class-distinguishing features were discovered in them, parameters for measuring them were formulated and implemented, and the resulting parameter values used for subsequent classification.

Three of these parameters were used as coordinates in a three-dimensional space. Each scan area was plotted in this three-dimensional parameter (or feature) space using the three parameter values, respectively, as the x , y , and z coordinates. Each scan area was assigned a letter, A , R , or N according to its classification as an agricultural, residential, or natural area. (Note, during this design phase, the scan areas were classified by us ahead of time, and the data for each area were so tagged within the computer.)

This three-dimensional space was explored to determine the distribution of the scan areas within it, the object being to establish criteria for separating the different categories. Fig. 33 shows a typical feature space plot as seen on the SARF console, and Fig. 34 shows some geometric decision boundaries injected into the plot. These boundaries were manipulated until separation of the categories were achieved.

To preserve the feature-extraction processing and the arrived-at decision boundaries, a logic decision tree is specified at the SARF console, as shown in Fig. 35.

To test the algorithm (now represented by the tree) all the data is "fed" into the tree, and the results collected in the form of a scoreboard, Fig. 36. The rows represent the actual categories, and the columns represent the tree output branches. All the agricultural and residential examples are

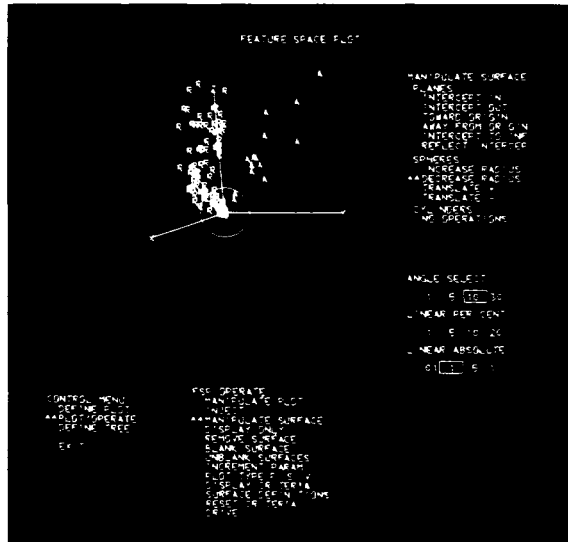


Fig. 33. Feature space plot on SARF console.

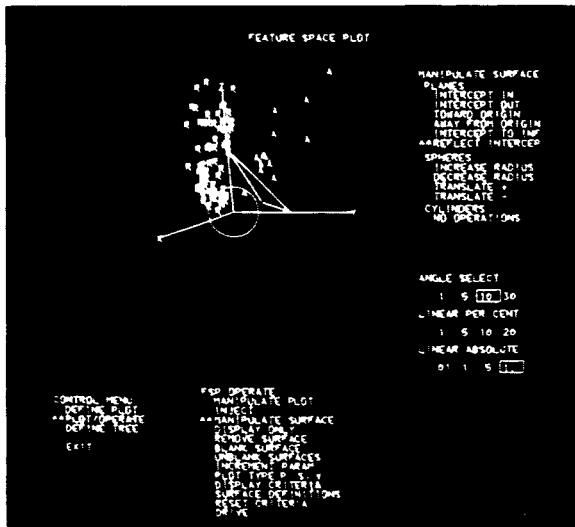


Fig. 34. Feature space plot with decision boundaries injected.

correctly classified, and all but one of the naturals are correctly classified.

For more details on this process, see [7]–[9].

Dimensional Information from Diffractograms

In another of our studies [6], we found that the FDP not only provides an excellent means for detecting regularity in a scan area, but it also provides dimensional information concerning both the object to be identified and, if the scan area contains an array of such objects, the lattice-like properties of the array. This kind of information concerning the pattern within the scan area can be important in an automatic pattern-recognition system in which clues are being assembled for pattern identification. This statement is based on the notion that, given the scale of the photograph and the general context of the area being scanned, the existence of and/or the dimension of regularity within the scan area is a very telling feature.

As an example of this notion, consider the collection of



Fig. 35. Logic decision tree.

Fig. 36. Algorithm results.

parked aircraft in the scan area shown in Fig. 37. The annular-ring signatures of these scan areas display a number of local peaks. Analysis of these signatures shows that the relative spacing of these peaks are directly related to the following:

- 1) nacelle separation,
 - 2) wing-to-stabilizer separation,
 - 3) wing and stabilizer lengths.

Further, because this FDP sampling was done with annular rings, this dimensional information is independent of the orientation or position of the parked aircraft.

In this example we note that the diffraction-pattern sampling technique serves for both object detection and ob-

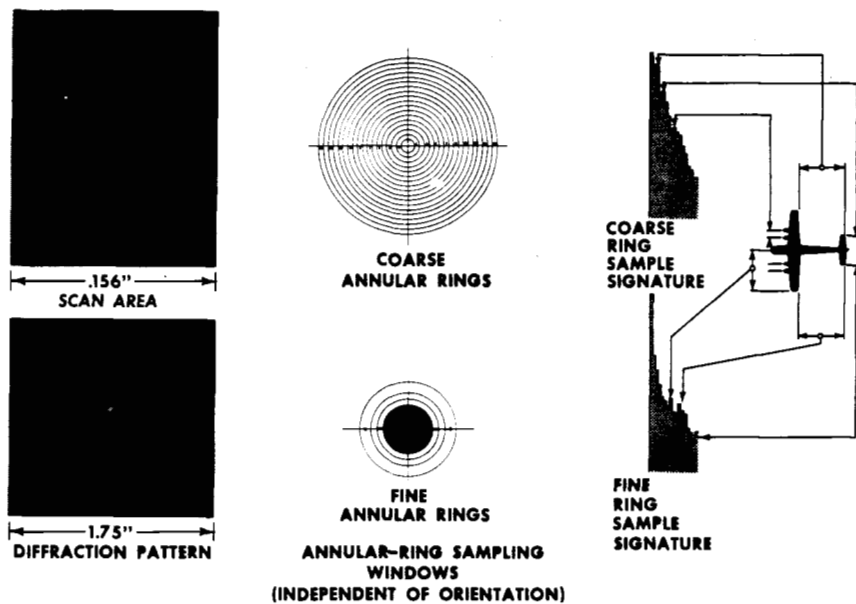


Fig. 37. Identification dimensions for aircraft extracted from sample signatures.

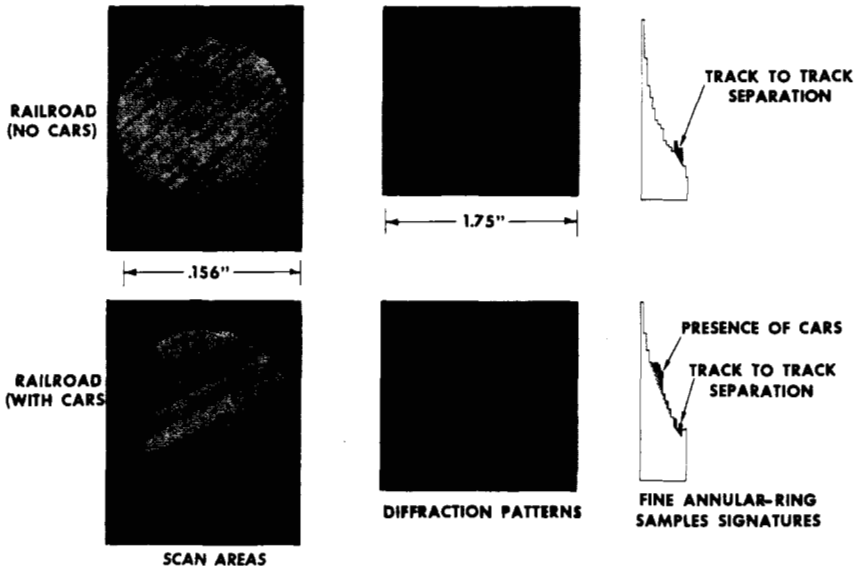


Fig. 38. Identification clues for railroads obvious in sample signatures.

ject identification. In addition, this example shows that even for a large collection of a given object (e.g., parked aircraft), identification can be made with only one set of measurements taken in parallel, in contrast to collating multiple measurements taken on each object in the group.

In addition to the annular-ring and wedge sample signatures, a technique was developed for measuring and recording a continuous intensity profile of an FDP in any direction and location. This was done by recording the light energy passing through a small aperture (called a fine probe) which traversed the FDP in the specified direction and location. In this way, having established the principal directions of information in an FDP (e.g., via a wedge sample signature) an intensity profile in that direction can be taken.

These were used to determine how well the annular-ring sample signatures captured the pertinent information,

and/or to obtain a higher resolution means of obtaining dimensional information concerning the object in the scan area. As an example, we compare Figs. 38 and 39.

Fig. 38 shows scan areas, diffraction patterns, and annular-ring sample signatures for railroad tracks with and without cars. Fig. 39 shows the frequency profiles of these FDPs along the direction indicated by line A. These frequency profiles clearly provide a higher resolution means of analyzing the FDP, and therefore provide more precise dimensional information concerning the objects in the scan area.

In the data acquired in this study, a high degree of correlation was achieved between object dimensions computed from the sample signatures and the corresponding dimensions measured directly from the photographs. It is significant that much of these data were derived from the annular-ring signatures, because this sampling is independent of

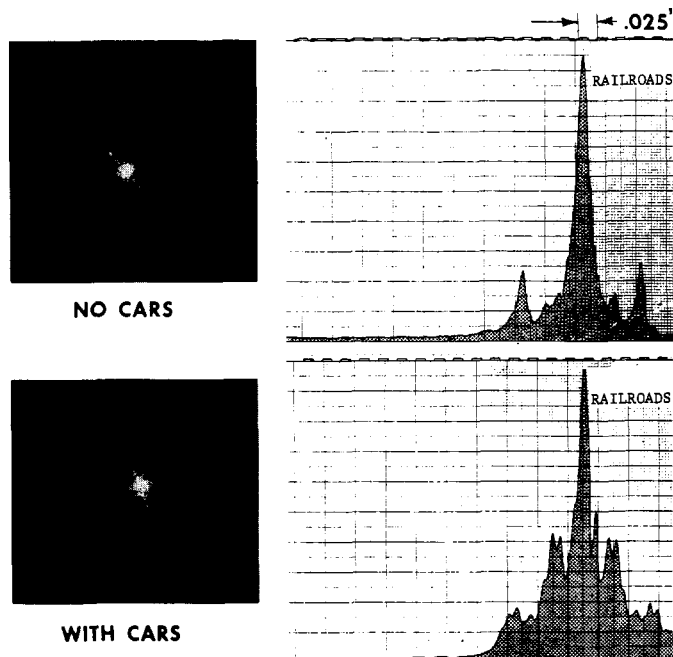


Fig. 39. Constant-direction intensity profiles for Fig. 38 scan-area diffraction patterns.

orientation (of either a single object, or relative orientation and location among a set of similar objects).

The experience acquired in this study suggested the following algorithm for extracting pertinent object signatures: 1) use annular-ring sampling for general frequency characteristics (especially for collections of objects); 2) use wedge sampling for determining angular relations and for selecting directions in which to obtain detailed intensity profiles; and 3) if appropriate, obtain the indicated profile plot or plots (particularly useful for single-object identification).

Many clues can be obtained by harmonic analysis of this frequency information, and these clues could be quite characteristic of specific object types, because they are directly related to the dimensions of the object. In addition, since the various dimensions of any given object (or object class) form certain fixed ratios, the derived characteristic frequency/harmonic relationships will be independent of scale. Adding this to the other properties of this technique results in a method that is basically independent of scale, translation, and rotation. Furthermore, the technique is one that could be implemented for extremely rapid parallel processing.

CONCLUSION

As mentioned several times in this paper, our investigations have shown that diffraction-pattern sampling can be a useful tool in effecting automatic pattern recognition in photographic transparencies. We do not mean to imply, however, that diffraction-pattern sampling can answer all the questions and problems associated with automatic pattern recognition.

Generally speaking, the design of an automatic pattern recognizer will depend very much upon the task to be performed. We do not believe that there is a general-purpose

automatic pattern recognizer (other than the human) in the offing for some time to come.

However, we do feel that we can learn a lot from the way humans do the job, and inject this into the design of automatic pattern-recognition algorithms. First of all, the human performs pattern recognition in a dynamic way. General information is sought first, and as information is obtained, or context is established, different types of information are sought, at each step more detailed, until the desired identification is made.

For example, in searching for a specific type of aircraft on the ground in an aerial photograph, a human, having first established the approximate scale, would scan the photograph very quickly to see if there are any linear features in it, and in particular those linear features which exhibit characteristics of airfields. Having found such an airfield, he will focus his attention (this time looking for details of a smaller scale) to looking for linear features characteristic of aircraft. Once he finds one or more aircraft, he then focuses his attention to looking for the specific kind he *had in mind*. If he finds one meeting this requirement, then his pattern-recognition task is completed.

For another example of the dynamic aspects of this process, consider the game of Twenty Questions. The contestant may ask any question of the type "is it x or not?" After each question is answered, the contestant formulates a new question and in this way proceeds, with up to 20 questions, to gather information to arrive at an answer. Those familiar with this game are well aware that it would be next to impossible to win this game if all 20 of the questions had to be asked before receiving any answers.

The human is able to win this game only because his experience in our environment has allowed him to build up a good model of that environment, and thus, by proper

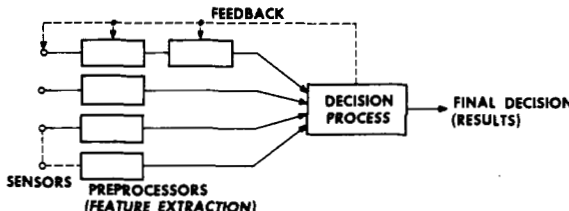


Fig. 40. General structure for an automatic pattern-recognition system.

questioning, can guide himself through the combinatorial tree of possibilities.

We believe that this kind of dynamic approach should be taken in the design of automatic pattern-recognition devices. The word 'dynamic' here is meant to imply the use of feedback, wherein the decision part of the device uses feedback to change the source and/or kind of information it receives (i.e., change the questions it is asking) as a function of its current state of knowledge. This, of course, implies that we must build into the decision maker a good model of the "environment" of the task it is to perform. A system structure of such a recognizer is shown in Fig. 40.

We feel that diffraction-pattern sampling can serve well as one of the preprocessors in such a system.

APPENDIX I

MATHEMATICAL DESCRIPTION OF SOME SAMPLING GEOMETRIES

If the amplitude transmission of the scan area is described by $t(x, y)$, and if the scan area is uniformly illuminated by a normally incident monochromatic plane wave, of amplitude A and wavelength λ , then the FDP formed by a spherical lens of focal length F is described by

$$T(\mu, v) = \frac{A}{\lambda F} \int_{-\infty}^{\infty} \int_{-\infty}^{\infty} e^{-2\pi i(\mu x + vy)} t(x, y) dx dy$$

where $\mu = (x_i/\lambda F)$, $v = (y_i/\lambda F)$, and x_i and y_i are coordinates in the transform (FDP) plane.

We recall that our sensors record the FDPMS, not the FDP. The FDPMS is described by

$$I(\mu, v) = T(\mu, v)T^*(\mu, v) = |T(\mu, v)|^2$$

where * denotes complex conjugate.

The sample signatures consist of a set of measurements (m_1, m_2, \dots, m_n) , where n is the number of sampling areas defined for the given sampling geometry.

For an annular-ring sampling geometry, the measurements are described by

$$m_j = \int_0^{2\pi} \int_{\rho_j}^{\rho_j + \Delta\rho} I(\rho, \theta) \rho d\rho d\theta, \quad j = 1, 2, \dots, n$$

where

$$\rho = \sqrt{\mu^2 + v^2} \quad \text{and} \quad \theta = \tan^{-1} \frac{v}{\mu}$$

Each of the m_j represent the total power in the band of spatial frequencies defined by

$$(\rho_j, \rho_j + \Delta\rho).$$

For a wedge sampling geometry, the measurements are described by

$$m_j = \int_{\rho_{\min}}^{\rho_{\max}} \int_{\theta_j}^{\theta_j + \Delta\theta} I(\rho, \theta) \rho d\theta d\rho, \quad j = 1, 2, \dots, n.$$

Each of the m_j represent the total power in the band of directions defined by $(\theta_j, \theta_j + \Delta\theta)$, for all frequencies larger than ρ_{\min} out to the limits of the measuring system (ρ_{\max}). To eliminate large zero-frequency contributions, ρ_{\min} is normally not set to zero.

For a slit sampling geometry, the measurements are described by

$$m_j(\theta) = \int_{-v_{\max}}^{v_{\max}} \int_{\mu_j}^{\mu_j + \Delta\mu} I(\mu, v) d\mu dv, \quad j = 1, 2, \dots, n$$

where the FDP is first rotated to a desired direction (an angle θ from some reference direction) before the measurements are taken. The height of the slit window ($2v_{\max}$) is arbitrary, but is normally determined by the extent of the FDP or the limits of the measuring system; the width of the slit window is $\Delta\mu$.

A frequency profile can be obtained along any desired direction (an angle θ from some reference direction) as follows.

$$m_j(\theta) = \int_{-v_a}^{v_a} \int_{\mu_j}^{\mu_j + \Delta\mu} I(\mu, v) d\mu dv, \quad j = 1, 2, \dots, n$$

where $2v_a$ is the height of the sampling window and $\Delta\mu$ is its width. For this case v_a and $\Delta\mu$ are generally small, while n is large, and the μ_j are selected for slight overlap of the samples.

This profile sampling can be generalized to perform a raster-scan sampling of the FDP. These measurements are described by

$$m_{jk} = \int_{v_k}^{v_k + \Delta v} \int_{\mu_j}^{\mu_j + \Delta\mu} I(\mu, v) d\mu dv \quad j = 1, 2, \dots, n_j \\ k = 1, 2, \dots, n_k$$

APPENDIX II

FUNCTIONAL DESCRIPTION OF GENERAL MOTORS' AC-DRL DPSS

As mentioned in the Introduction, the implementation of FDP sampling at AC-DRL has undergone a two-step evolution from that described in [4], the last step being an automated Diffraction Pattern Sampling System (DPSS).

The following is a functional description of the DPSS. DPSS can be controlled manually by way of a control panel provided for the operator, or it can be operated in a completely hands-off mode by the computer system to which it is attached.

In the following description, reference is made to Fig. 41.

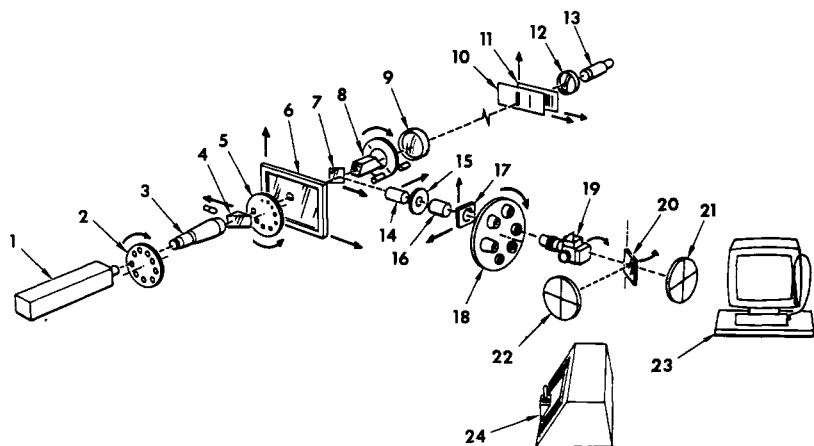


Fig. 41. Schematic of General Motors' AC-DRL diffraction-pattern sampling system.

Item Number	Item Name	Description and/or Function	Item Number	Item Name	Description and/or Function
1	Laser	Provides monochromatic, coherent light for generating the diffraction pattern.	10*	Sample window selector plate	This is moved in relation to the plate at 11 to select one of the windows on that plate. While sampling, the two plates are moved together. They are both under computer control, and the stepping increments are nominally 0.001 inch.
2*	Intensity control disk	Contains neutral density filters of different densities. Used to control the laser light intensity.	11*	Sample window plate	A photographic plate, all opaque with the exception of various sample windows. A window is selected by 10, and both windows are moved to the optical axis; then appropriate motions are made according to the sampling desired.
3	Beam expanding and collimating optics	Used to generate a 20-mm or 50-mm collimated light beam. Includes a pin hole spatial filter to "clean up" the beam.	12	Collection lens	Collects all the light energy coming through the sampling window and focuses it onto the photo detector 13.
4	Prism	This is moved in and out of the optical path. When out of the path, the laser illuminates the film 6; when in the path, a white light source illuminates the film.	13	Photo detector	A photomultiplier tube with an S-20 photocathode. The output is fed to an extended range integrator which has a linear range of nearly 5 decades. The output of the integrator is converted and sent to the computer via a data control unit.
5*	Aperture disk	Provides variable scan-aperture capability. Contains a sequence of different apertures ranging in size from 0.040 inch diameter to 0.596 inch diameter used when sampling, and one aperture of 1.00 inch diameter for context viewing. These apertures determine the size of the laser beam illuminating the film plate—hence, they determine the size of the scan area.	14	Relay lens 1	This is moved in and out of the optical path. When in the path, the scan area is projected onto 19, 21, or 22; when out, the diffraction pattern is projected onto 19, 21, or 22.
6*	Film holder	The film is mounted on a digitally driven, two-axis table. Any location on a 9 by 9 inch film can be positioned on the optical axis. This determines the center of the scan area; the diameter of the scan area is determined by the aperture selected 5. The position of the table can be controlled either manually via the joystick, or directly by the digital computer.	15	Iris	Controls the intensity of the projected images at 21 and 22.
7	Mirror	This is moved in and out of the optical path. When in the path, the viewing portion of the system is selected; when out, the sampling portion of the system is selected.	16	Relay lens 2	This is part of the lens system to accomplish the projections described in 14.
8*	Dove prism	The dove prism rotates the diffraction pattern for the purpose of generating certain of the sample window sets. It is driven, selectively, by either a digital stepping motor or a continuous motor.	17	Spatial filter holder	Has both rotational and X, Y motion capability (under manual control) and is used for spatial filtering experiments.
9	Lens	This forms the Fourier transform of the scan area at the plane defined by 11.	18	Lens turret	Brings (under manual control) the appropriate optics into the optical path to make the projections (of the scan area or diffraction pattern) at 21 or 22 either 10×, 20×, 50×, or 100×.
* These units are under computer control, and can be utilized as part of a dynamic pattern-recognition algorithm.					
(continued)					

Item Number	Item Name	Description and/or Function
20	Mirror	This is moved in and out of the optical path. When in the path, the projection is at screen 22; when out, the projection is at screen 21.
21, 22	Projection screens	Rotatable projection screens with crosshairs, and a ruling engraved on one axis.
23	Computer graphics console	DPSS can be controlled from the SARF graphics console, via the computer. The analyst "flies" over the film (using the joystick of 24), views it on screen 21, selects the scan-areas he wishes to sample, and by light-pen selecting appropriate instructions on the display, initiates automatic transfer of their coordinates on the film plate into the computer. He then classifies the scan areas by light-pen selecting the appropriate name from a list of categories which appears on the display console. The selected scan areas with their corresponding identification tags are compiled into a list in the computer. This list is used later by the computer in effecting an automatic sampling of the FDPs of the selected scan areas. Proximity of the console to screen 21 allows the analyst to relate the contents of the scan area and its FDP (viewed on screen 21) to the sample signatures, to the features derived therefrom, and to any other processing displayed on the graphics console during his algorithm design sessions on SARF.
24	Control panel	This control panel allows the operator to operate DPSS for noncomputer experiments.

REFERENCES

- [1] J. W. Goodman, *Introduction to Fourier Optics*. San Francisco, Calif.: McGraw-Hill, 1968.
- [2] M. Born and E. Wolf, *Principles of Optics*. New York: Pergamon, 1959.
- [3] F. W. Sears, *Optics*. Cambridge, Mass.: Addison-Wesley, 1949.
- [4] G. G. Lendaris and G. L. Stanley, "An optical self-organizing recognition system," in *Optical and Electro-Optical Information Processing*. Cambridge, Mass.: M.I.T. Press, 1965, ch. 29.
- [5] —, "Interpreting aerial photography with the GM-DRL pattern recognition system," General Motors AC-Defense Res. Labs., Santa Barbara, Calif., Tech. Rept. TR65-91, January 1966.
- [6] —, "Applications of diffraction-pattern sampling to automatic target recognition," General Motors AC-Defense Res. Labs., Santa Barbara, Calif., Tech. Rept. TR67-06, January 1967.
- [7] "The application of SARF/DPSS to the development of an ATR system," General Motors AC-Defense Res. Labs., Santa Barbara, Calif. Publ. no. S68-10, July 1968.
- [8] "SARF, signature analysis research facility," General Motors AC-Defense Res. Labs., Santa Barbara, Calif., Publ. no. S68-11A, October 1968.
- [9] G. L. Stanley, W. C. Nienow, and G. G. Lendaris, "SARF, an interactive signature analysis research facility," General Motors AC-Defense Res. Labs., Santa Barbara, Calif., Tech. Rept. TR69-15, March 1969; also *Proc. Purdue University Centennial Year Symp. on Information Processing*, 1969.

For further information the following were suggested by the reviewers.
 A. Papoulis, *Systems and Transforms with Applications in Optics*. New York: McGraw-Hill, 1968.

C. A. Taylor and H. Lipson, *Optical Transformation*. Ithaca, N. Y.: Cornell University Press, 1964.

"Fourier-transform methods for pattern recognition," Air Force Cambridge Res. Lab., Cambridge, Mass., July 1962.

Asendorf, "Pictorial pattern recognition," in *Proc. Symp. on Automatic Photo Interpretation*, Washington, D. C.: Thompson Books, 1969, ch. 10.

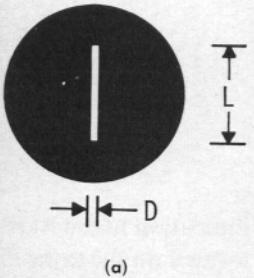


Fig. 3. (a) Rectangular aperture. (b) FDPMS of (a).

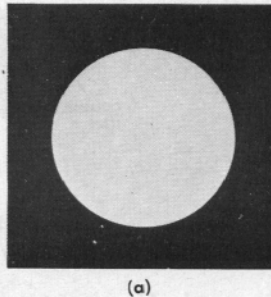
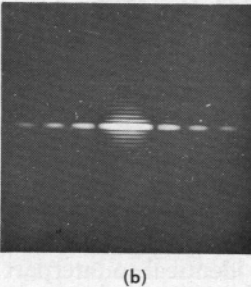
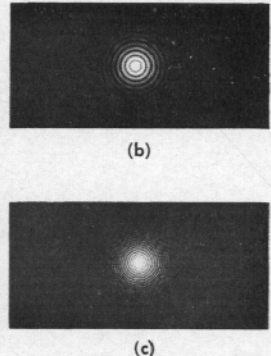
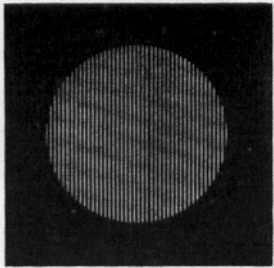
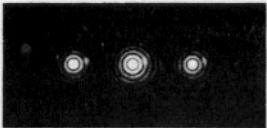


Fig. 5. (a) Circular aperture. (b) FDPMS of (a) with radius R .
(c) FDPMS of (a) with radius $2R$.

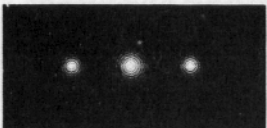




(a)

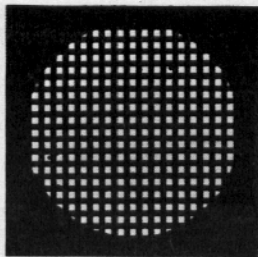


(b)

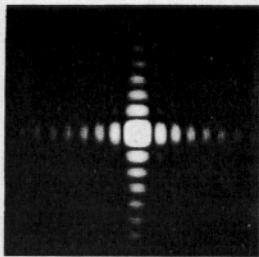


(c)

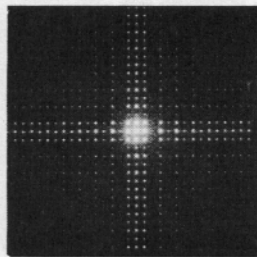
Fig. 7. (a) Parallel lines through a circular aperture. (b) FDPMS of a grating through radius R . (c) FDPMS of a grating through radius $2R$.



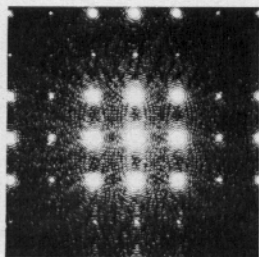
(a)



(b)

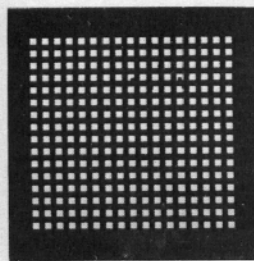


(c)

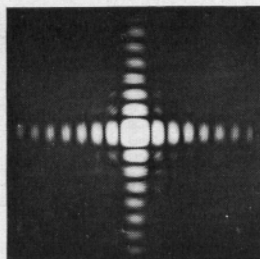


(d)

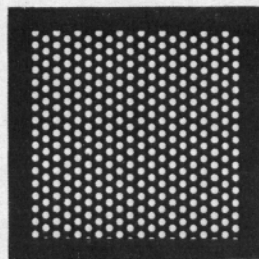
Fig. 8. (a) Array of rectangles through a circular aperture. (b) FDPMS of one of the rectangles of (a). (c) FDPMS of (a). (d) Center portion of (c).



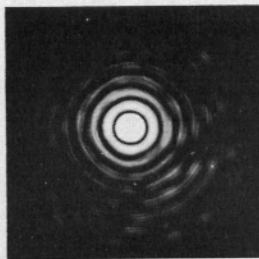
(a)



(b)

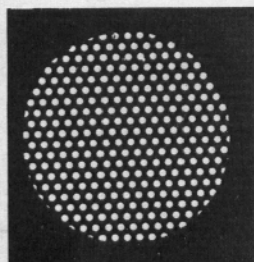


(c)

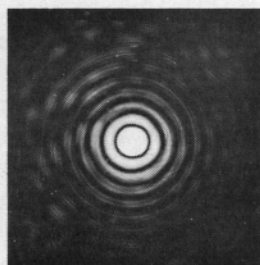


(d)

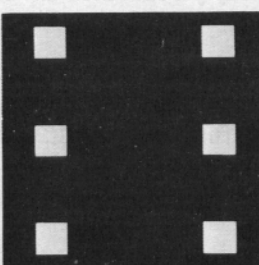
Fig. 9. (a) Array of rectangles through a rectangular aperture. (b) FDPMS of one of the rectangles of (a). (c) FDPMS of (a). (d) Center portion of (c).



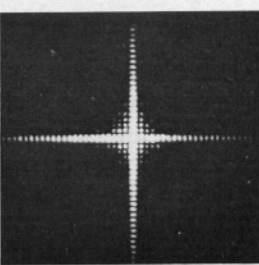
(a)



(b)

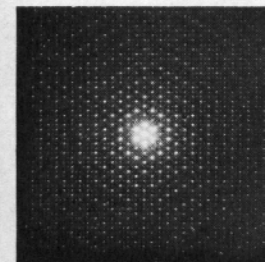


(c)

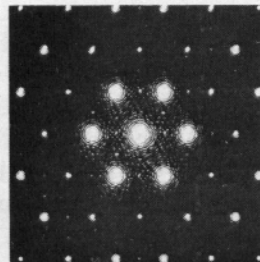


(d)

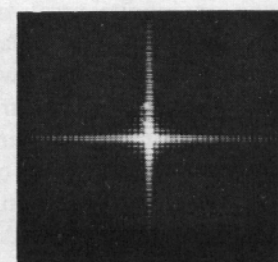
Fig. 10. (a) Array of circles through a circular aperture. (b) FDPMS of one of the circles of (a). (c) FDPMS of (a). (d) Center portion of (c).



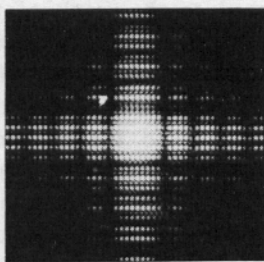
(a)



(b)

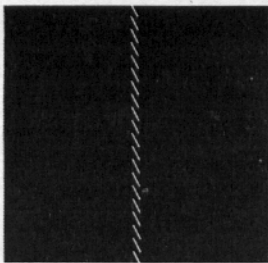


(c)

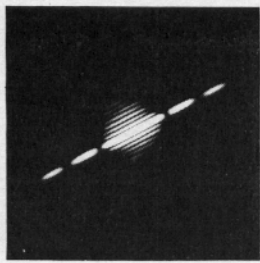


(d)

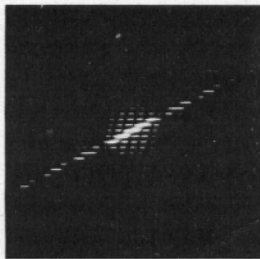
Fig. 12. (a) Array of six squares. (b) FDPMS of one of the squares of (a). (c) FDPMS of (a). (d) Center portion of (c).



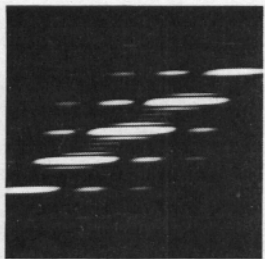
(a)



(b)

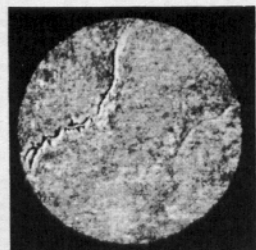


(c)

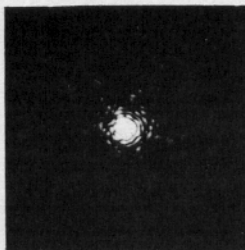


(d)

Fig. 13. (a) Staggered rectangular objects (similar to parked cars). (b) FDPMS of one of the rectangles of (a). (c) FDPMS of (a). (d) Center portion of (c).

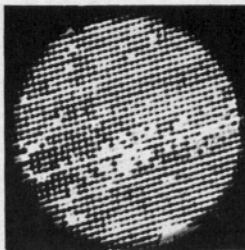


(a)

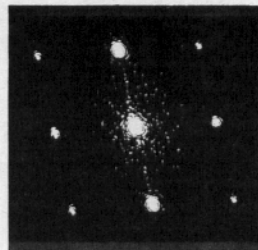


(b)

Fig. 15. (a) Natural terrain. (b) FDPMS of (a).

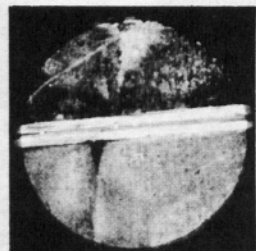


(a)

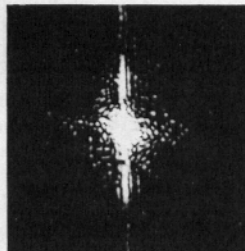


(b)

Fig. 18. (a) Orchard. (b) FDPMS of (a).

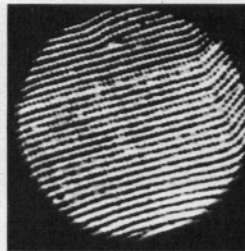


(a)



(b)

Fig. 16. (a) Roadway with natural terrain background. (b) FDPMS of (a).

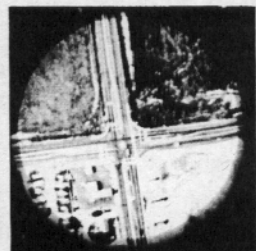


(a)

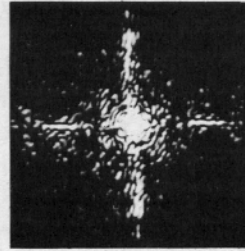


(b)

Fig. 19. (a) Orchard on hillside. (b) FDPMS of (a).

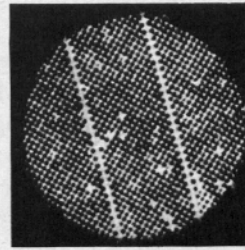


(a)

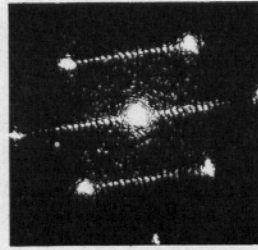


(b)

Fig. 17. (a) Road intersection. (b) FDPMS of (a).

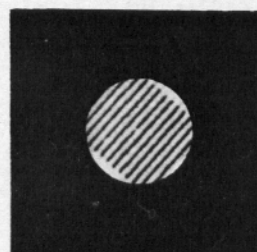


(a)

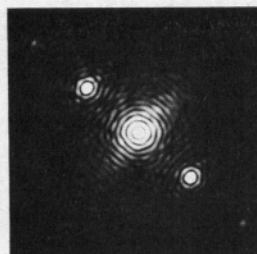


(b)

Fig. 20. (a) Orchard with service roads. (b) FDPMS of (a).

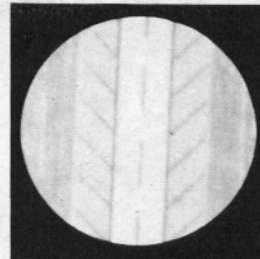


(a)

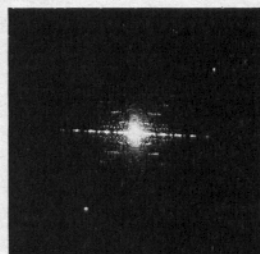


(b)

Fig. 21. (a) Vine crop. (b) FDPMS of (a).

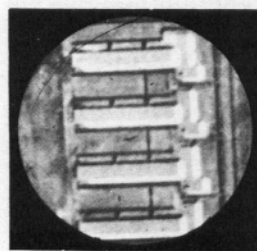


(a)

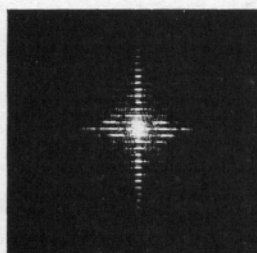


(b)

Fig. 24. (a) Runway strip with chevrons. (b) FDPMS of (a).

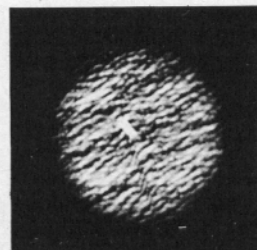


(a)

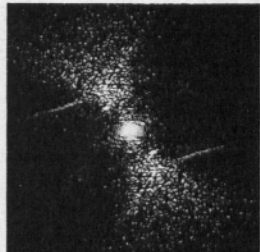


(b)

Fig. 22. (a) Complex of large buildings. (b) FDPMS of (a).

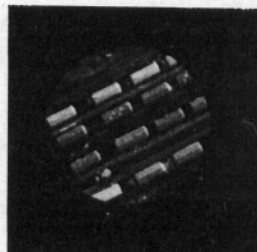


(a)

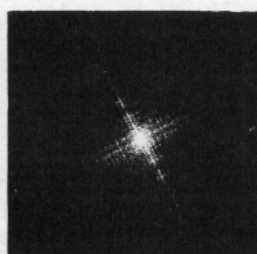


(b)

Fig. 25. (a) Ship at sea and wake. (b) FDPMS of (a).

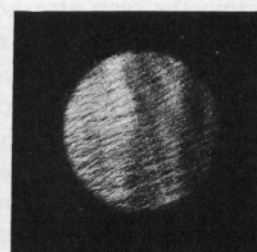


(a)

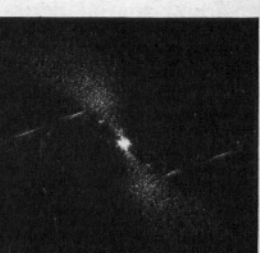


(b)

Fig. 23. (a) Complex of smaller buildings. (b) FDPMS of (a).



(a)



(b)

Fig. 26. (a) Ship wake and ocean surface. (b) FDPMS of (a).

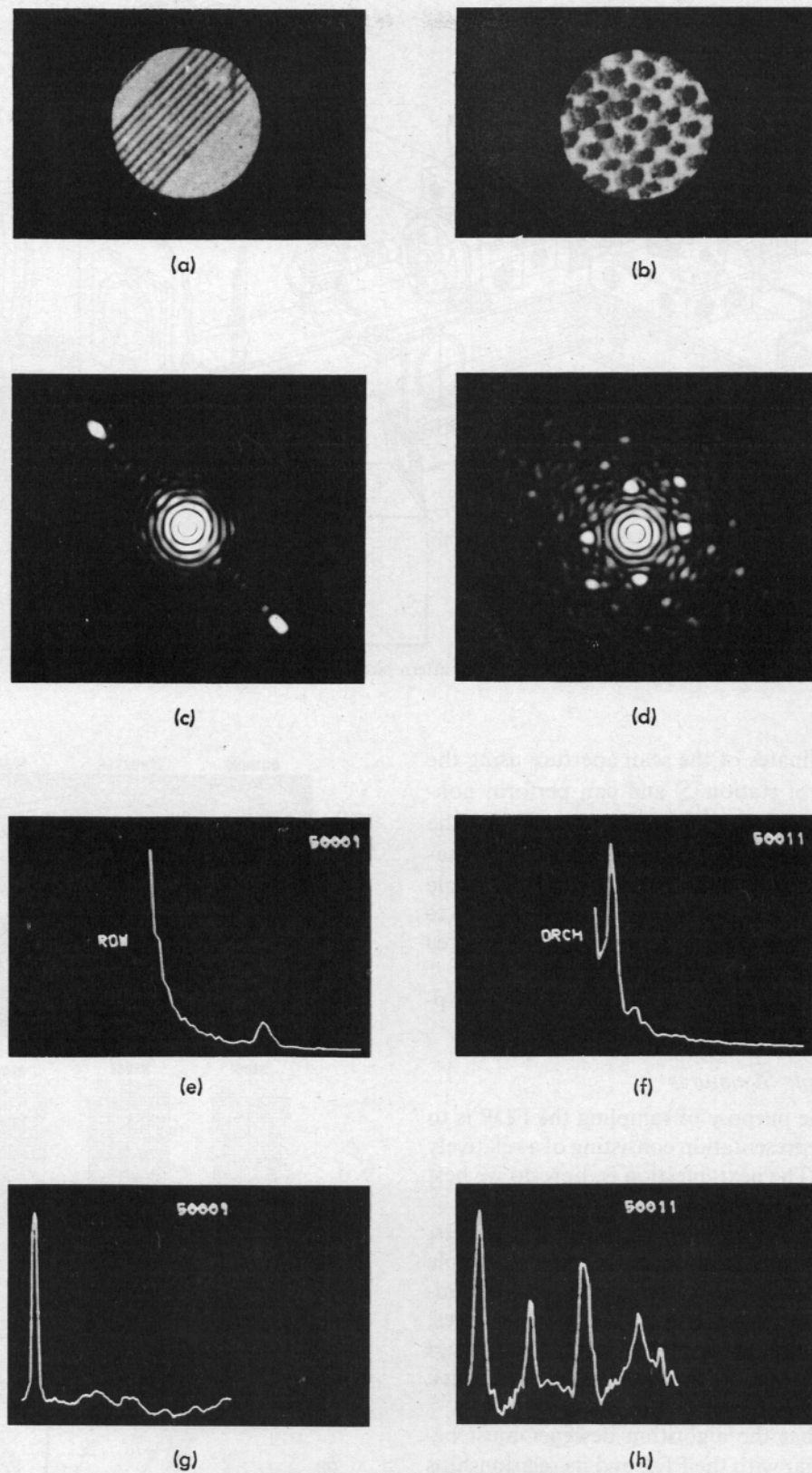


Fig. 28. (a) Agriculture one-dimensional periodicity. (b) Agriculture two-dimensional periodicity. (c) FDPMS of (a). (d) FDPMs of (b). (e) Annular-ring sample signature of (c). (f) Annular-ring sample signature of (d). (g) 1.8° wedge sample signature of (c). (h) 1.8° wedge sample signature of (d).

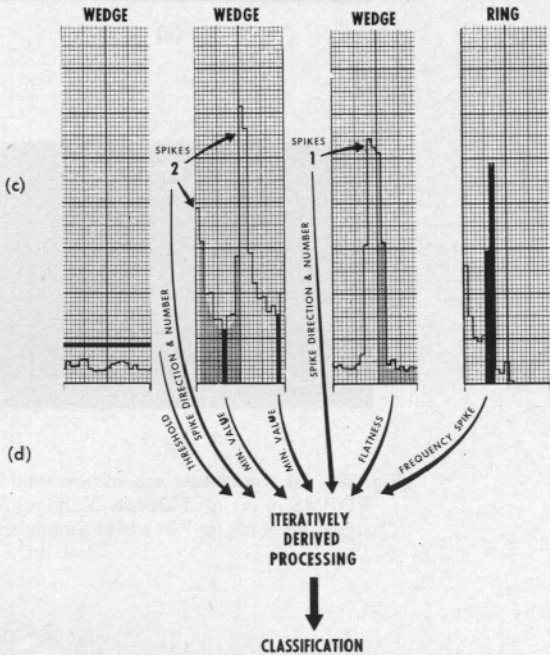
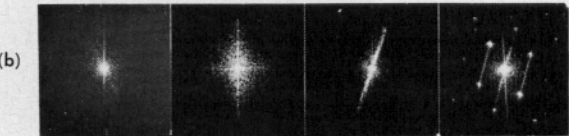
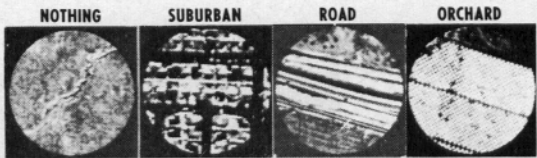


Fig. 30. Classification process.

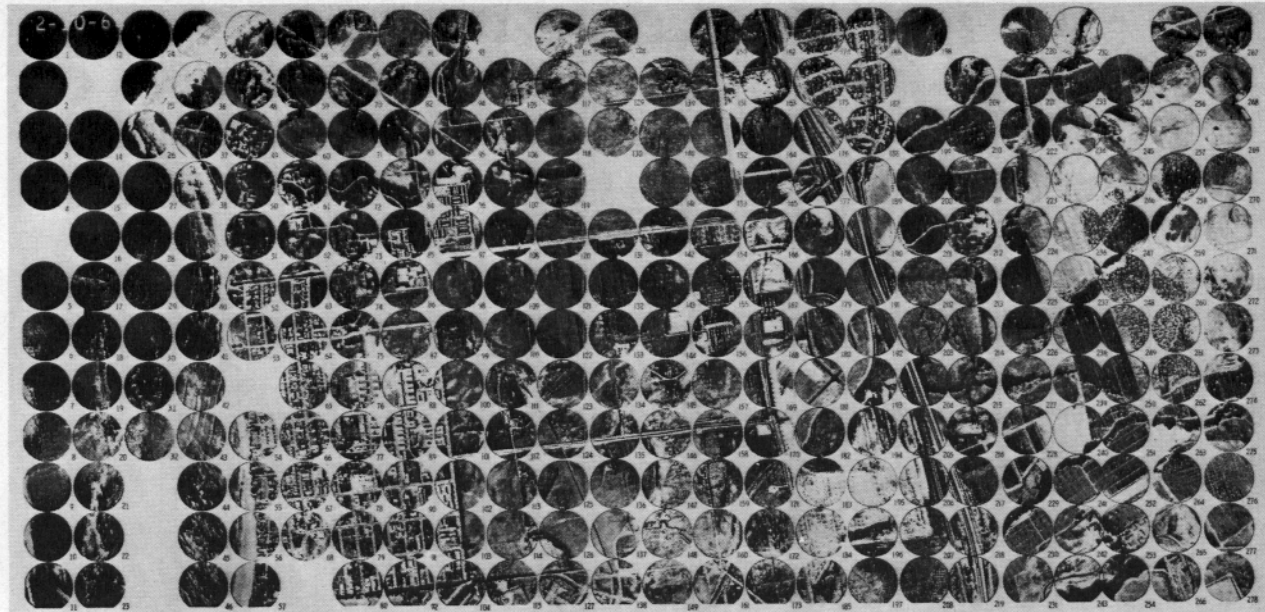


Fig. 31. Aerial photograph of Goleta Valley with scan-area selections indicated.

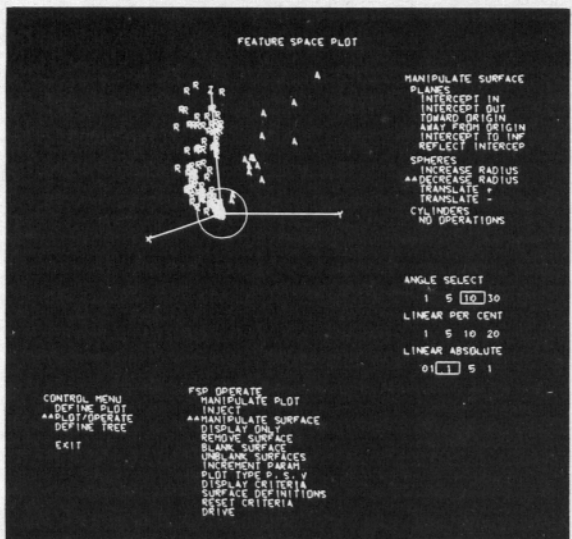


Fig. 33. Feature space plot on SARF console.

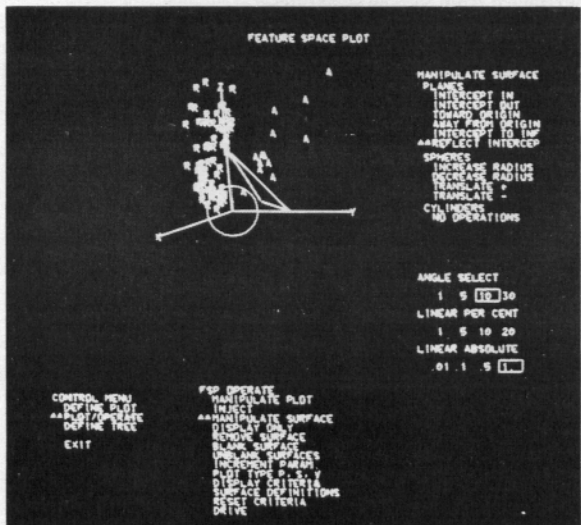
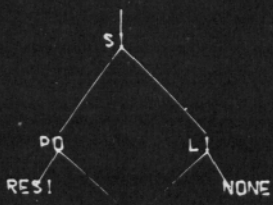


Fig. 34. Feature space plot with decision boundaries injected.

FEATURE SPACE PLOT



OR
FARM

CONTROL MENU

- DEFINE PLOT
- PLOT/OPERATE
- **DEFINE TREE**
- EXIT

DEFINE TREE

- DEFINE NODE L, P, S
- PLACE NODE
- LINK NODE
- REMOVE LINK
- MOVE NODE
- REMOVE NODE
- REDEFINE NODE
- COMPUTE
- **NAME BRANCH**
- COMPACT

Fig. 35. Logic decision tree.

TEST & EVALUATE

	FARM	RESI	NONE	XXXX	XXXX	XXXX	XXXX	XXXX
AGR1	11	0	0					
RES1	0	68	0					
NATU	0	1	51					
XXXX								
XXXX								
XXXX								
XXXX								
XXXX								
XXXX								
XXXX								
XXXX								
XXXX								

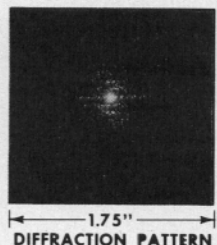
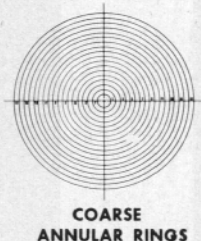
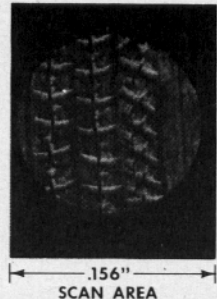
CONTROL MENU

- DEFINE MATRIX
- **COMPUT MATRIX**
- EXIT

COMPUTE MATRIX

DRIVE

Fig. 36. Algorithm results.



ANNUAL-RING SAMPLING
WINDOWS
(INDEPENDENT OF ORIENTATION)

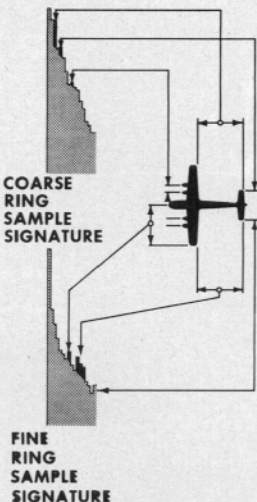
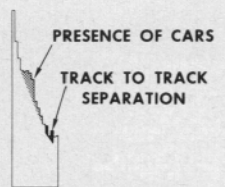
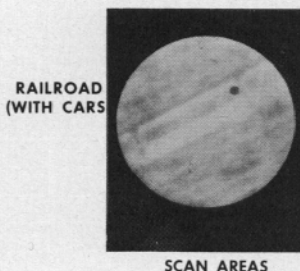
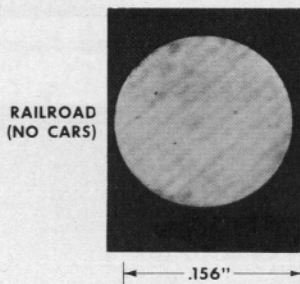
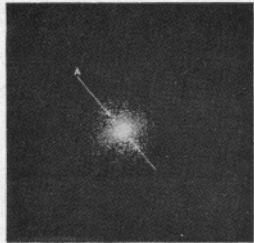


Fig. 37. Identification dimensions for aircraft extracted from sample signatures.

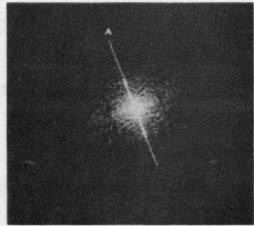


FINE ANNULAR-RING
SAMPLES SIGNATURES

Fig. 38. Identification clues for railroads obvious in sample signatures.



NO CARS



WITH CARS

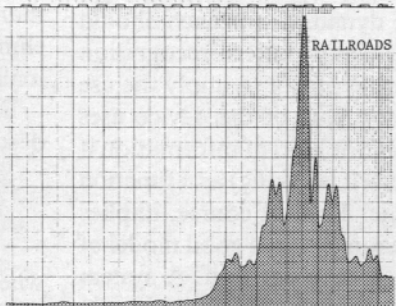
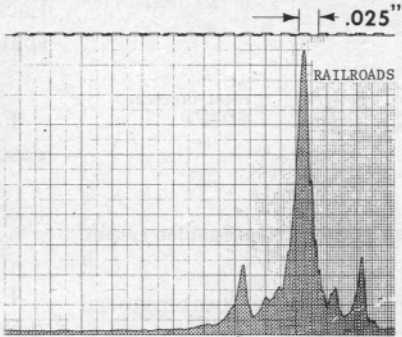


Fig. 39. Constant-direction intensity profiles for Fig. 38 scan-area diffraction patterns.